Catheter with Improved steerability for the TAVI Procedure

Design, Development and Validation

Luuk Schouten

Technische Universiteit Delft

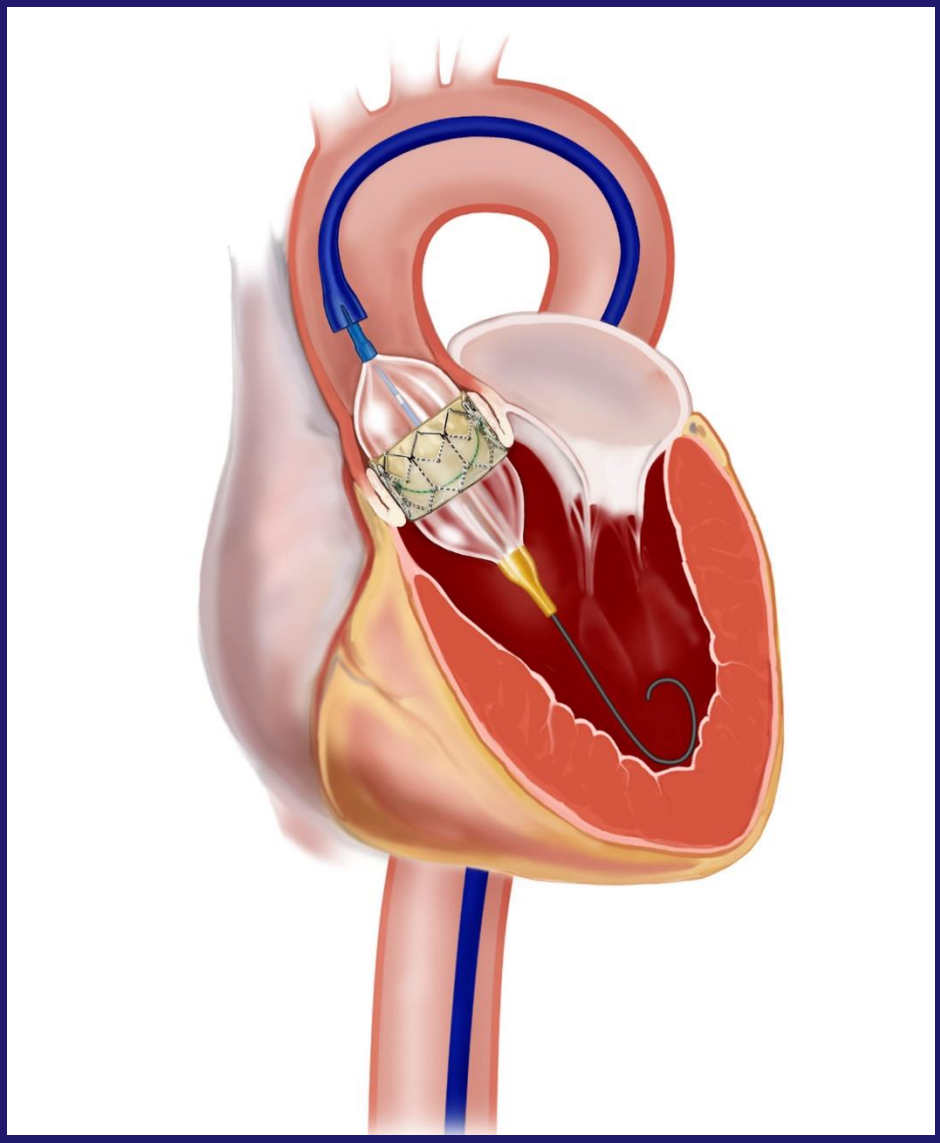

TU Delft Delft University of Technology

Challenge the future

Catheter with Improved steerability for the TAVI Procedure

Design, Development and Validation

by

Luuk Schouten

in partial fulfillment of the requirements for the degree of

Master of Science
in Biomedical Engineering

at the Delft University of Technology,
to be defended publicly on Friday September 22, 2017 at 14:00.

Supervisor:	Dr. J. van den Dobbelsteen	
Thesis committee:	Prof. dr. J. Dankelman,	TU Delft
	Dr. J. van den Dobbelsteen,	TU Delft
	Dr. ir. R. Mugge,	TU Delft

TU Delft Delft University of Technology

Acknowledgements

Allereerst wil graag mijn begeleider John van den Dobbelsteen bedanken voor zijn hulp in dit afstudeerproject. Nadat ik had verteld naar wat voor een soort project ik op zoek was, legde hij dit onderwerp voor. Dit voldoet aan mijn wensen om een technische oplossing te vinden voor een klinisch probleem. Gedurende het proces kreeg ik veel vrijheid, maar waren er een aantal momenten dat er een duw in de goede richting nodig was. Tijdens meetings kreeg ik hiervoor de nodige feedback en dat heeft er voor gezorgd dat het project binnen de tijdsmarge naar een goed einde is gebracht.

Graag wil ik Jenny bedanken voor de feedback gedurende dit master project. Daarnaast wil ik je ook bedanken voor de connectie met Ecuador waardoor ik daar uiteindelijk mijn stage heb mogen doen. Ik kijk hier met veel plezier op terug.

Vervolgens wil ik mijn vrienden bedanken hier aan de TU Delft. Het begon allemaal bij de Study Tour en hier hebben we elkaar goed leren kennen. Door elkaar scherp te houden tijdens onze studie carrière hebben we het laatste jaar snel richting een einde kunnen brengen. Jullie hebben me ook geholpen met de zoektocht naar een baan en van de nodige feedback voorzien voor het sollicitatieproces. De verschillende reisjes en borrelavonden gaan de geschiedenisboeken in en ik kijk uit naar de toekomstige plannen. Daarnaast wil ik in het bijzonder Manon bedanken voor alle support tijdens de laatste fase van mijn studie.

Tot slot, wil ik mijn ouders bedanken die mij deze gehele rit hebben gesteund. Jullie hadden altijd een luisterend oor als ik het nodig had en stonden voor mij klaar als er bijvoorbeeld weer eens verhuisd moest worden. Ik ben jullie dankbaar voor alle waarden die jullie me hebben meegegeven en alle vrijheid die jullie me hebben gegeven sinds ik voor het eerst op eigen benen ging staan. Het kind is afgeleverd en ik ben er enorm tevreden mee. Bedankt voor alles!

Abstract

Aortic stenosis is one of the most serious heart valve diseases and is the result of calcification of the aortic valve leaflets. This calcification is irreversible and negatively affect the functionality of the heart valves. The only treatment is an aortic valve replacement. The trend in heart valve replacement is moving from open heart surgery towards minimally invasive techniques where a heart valve prosthesis is placed over the native aortic valve, called the TAVI procedure.

A crimped stent that contains a heart valve prosthesis is pushed upwards through the femoral access route with a delivery catheter. This prosthesis is placed in the aortic annulus and wedged over the native valve. The positioning of the heart valve prosthesis is important for the success of the procedure and durability of the prosthesis. A coaxial placement to the aortic annulus in the center of the aorta lumen is the target during this positioning of the prosthesis.

The Medtronics and Edwards delivery systems, that are currently used, only have the possibility to be steered with a maximum of 1 rotation, providing an alignment with the aortic annulus in the frontal plane of the body. The rotation to provide the alignment in the sagittal plane is lacking. This report will focus on the question if extra steerability of the delivery system will provide a better positioning of the tip of the delivery system, which in the end, will position the heart valve prosthesis.

The Edwards delivery system will be reverse engineered to look at the current mechanisms that are used to provide the rotation in the frontal plane. Subsequently, two experiments are performed to select the best configuration for the modification on the tip of the delivery system. Ultimately, the designed prototype will be validated with two tests to answer the research question if the extra steerability will provide a better positioning.

The prototype is validated by comparing the positioning of the Medtronics and Edwards delivery system with the prototype during an experiment where the three systems have to be maneuvered to a predefined position in an aorta model of glass. This predefined position represents the center of the aorta lumen in a coaxial oriëntation. Two rotations and the xyz-coordinations of the tip will be measured by an Aurora NDI system and the results will be compared.

It showed that the prototype provided a bigger reach within the aorta lumen and a had a bigger domain of angles in which the tip could be oriëntated than the prototype. Moreover, the prototype provided a better alignment in the sagittal and frontal plane with regards to the reference point.

The research only focused on the positioning of the tip and didn't take the deployment of the heart valve prosthesis into account. Further development of the prototype is needed to make it usefull for the TAVI procedure. In addition, more research is needed to validate the prototype in a dynamic environment that represents the reality with blood flow and more tortuosity in the access route. Nevertheless, the prototype look promising to be used for the perfect positioning of the heart valve prosthesis which will have a positive effect on the durability and functionality of the prosthesis.

Contents

1

General introduction

Aortic stenosis (AS) is one of the most common and most serious valve disease problems [14]. The prevalence of aortic stenosis increases with age and is fatal within 2-3 years from symptom onset if left untreated [11, 36]. It's the result of calcification of the leaflets of the aortic valve. The difference between a healthy aortic valve and a valve that is affected by stenosis is visible in figure 1.1.

During the cardiac cycle a heart valve acts as follows. The heart valve opens completely when the left ventricle contracts, to ensure outflow of oxygen rich blood into the aorta. When the left ventricle is completely contracted and the pressure in the left ventricle is lower than the pressure in the aorta, the aortic valve closes to prevent blood from flowing backwards into the ventricle [18]. When the function of the valve is affected, the function as is described above is affected. The stenosis causes a narrowing of the valve that is visible in figure 1.1. This narrowing causes more resistance and turbulence distal to the valve, resulting in a pressure drop. The anatomical effects can be a thickening of the left ventricular and left atrial wall because the heart wants to compensate for this pressure loss [18]. People can experience breathlessness, chest pain, a feeling of heavy heartbeats or heart murmer because of theses effects.

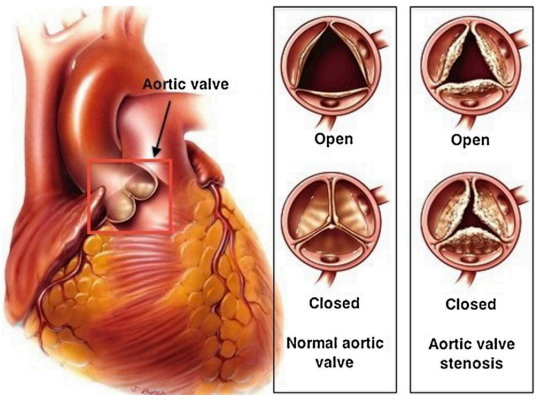

Figure 1.1: Normal aortic valve on the left and aortic valve stenosis on the right. The normal aortic valve opens fully to let oxygen-rich blood flow from the left ventricle into the aorta. Between beats, the aortic valve closes to keep blood from flowing backward into the heart. With aortic valve stenosis, because the valve does not open as wide, the heart must work harder to pump blood through the valve [7]

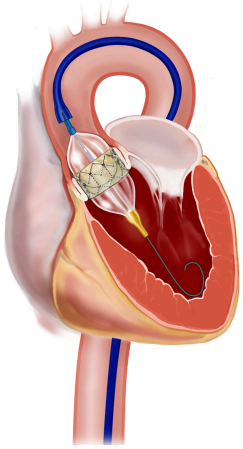

Figure 1.2: TAVI procedure wherein a heart valve prosthesis is placed over the native aortic valve whilst delivered by a catheter (image from http://www.papworthhospital.nhs.uk).

There is no medication that reverses the effect of calcification and the valve has to be replaced to treat this condition. Open heart surgical aortic valve replacement is still the standard treatment for this condition. The medically ill population don't tolerate this treatment well, because the recovery from this

Figure 1.3: The two delivery systems with on the left hand side the Medtronics DS with the unfolded Corevalve. This stent is crimped into the tip of the DS as the figure illustrates. On the right hand side the Edwards DS is visible with the prosthesis surrounding the balloon, illustrating how the tip of the DS can be steered.

procedure asks a lot from the body [15]. That is why the trend in heart valve replacement is moving toward minimally invasive implantation called the transcatheter aortic valve implantation (TAVI)to avoid this complicated open heart surgery [4]. This procedure uses a minimally invasive technique where an aortic valve prosthesis is implanted over the native aortic valve that suffers from symptomatic aortic stenosis, see figure 1.2.

This percutaneous technique uses a delivery system mounted with a crimped valve prosthesis at the distal tip of the delivery system (DS). The DS is manoeuvred through the transfemoral access route and when the distal tip with the prosthesis is positioned correctly, the stent is wedged over the native aortic valve. The whole procedure including the assessment and evaluation that is needed to determine the anatomy and tortuosity of the access route to the aortic valve is explained in more detail in appendix 5.1.

Currently, two valve prosthesis are approved for the TAVI procedure and mainly used. The Edwards Sapiën XT™ (Edwards Lifesciences, Irvine, CA, USA) and the Medtronic CoreValve™ Revalving system (Medtronic Inc, Minneapolis, MN, USA), depicted in figure 1.3. The Edwards prosthesis consists of a balloon-expandable cobalt chromium stent frame with a trileaflet bovine xenovalve. The Medtronic Corevalve consists of a porcine trileaflet valve mounted within a Nitinol self-expanding stent frame [34]. The prosthesis are deployed with delivery systems that are specifically designed for each valve prosthesis. The Medtronic Corevalve has a DS that allows rotation in one plane, visible in figure 1.3. The Edwards Sapiën valve has a DS that is steerable with one rotation, visible in figure 1.3.

Figure 1.4 shows the anatomy of the aorta of the human body. The delivery systems enter the body in the iliac artery and are pushed upwards through the aorta to the aortic annulus, which is located between the aorta and the left ventricle [18]. A coaxial positioning of the tip of the delivery system en subsequently the prosthesis is very important for the success of the implantation (see Appendix 5.3). Misplacement can lead to aortic regurgitation, shortening of the lifespan of the prosthesis, embolization and dislocation of the prosthesis. The direct access during open heart valve replacement makes it straightforward to navigate the aortic valve prosthesis to the correct position. The navigation of the aortic valve with a catheter over a longer distance makes it more difficult to deploy the aortic valve on the correct position [15].

Figure 1.5 shows the two rotations that have to be challenged during the placement of the heart valve prosthesis. The Medtronics DS allows rotation A when it is pushed upwards and the self expanding stent is designed to center itself in the aortic annulus when deployed. In addition, the Edwards DS can be steered providing rotation A in order that the tip can be aligned in the frontal plane of the aortic annulus. However, the aortic annulus is a 3D structure where it is also possible that there is a rotation in the sagittal plane illustrated by rotation B in figure 1.5 (see appendix 5.2). The current delivery systems lack the possibility to steer the distal tip in a coaxial alignment in the sagittal plane and that is where this research will focus on.

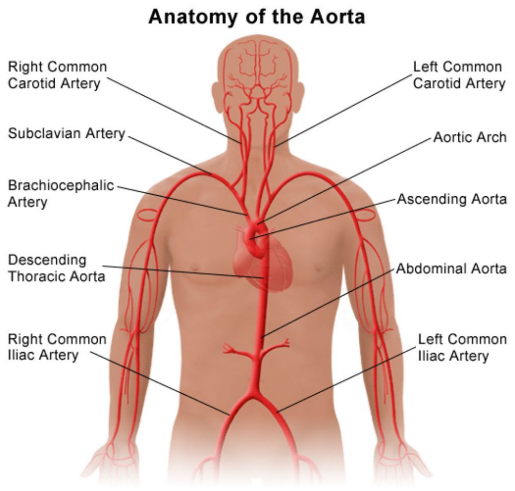

Figure 1.4: The anatomy of the aorta in the human body showing the route from the iliac artery, which is the starting point for the TAVI procedure, to the aortic annulus.

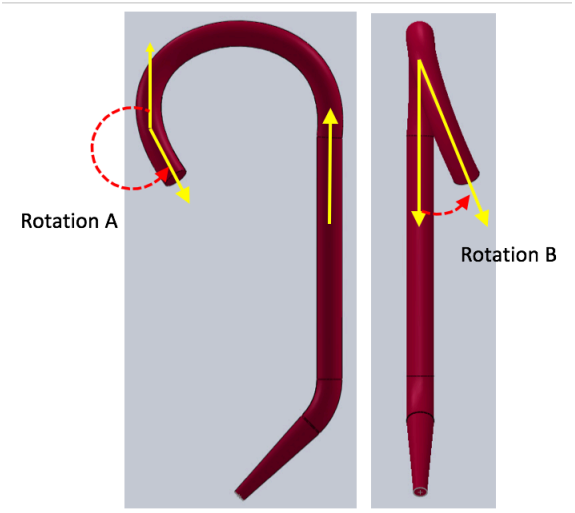

Figure 1.5: A simplified model of the route from the iliac artery to the aortic annulus with on the left hand side a frontal view and on the right hand side a sagittal view. The two rotations that are referred to in this research are depicted as rotation A and rotation B.

1.1. Problem description

The valve placement in the TAVI procedure comes with more variability compared to an open heart surgical procedure [15]. The direct access during open heart valve replacement makes it easier to navigate the aortic valve to the correct position. The navigation of the aortic valve with a catheter over a longer distance makes it more difficult to deploy the aortic valve on the right position. The challenge that comes with the TAVI method is to provide steerability in the appropriate location in the distal extremity of the catheter while maintaining the rigidity in the proximal part [16].

Coaxial positioning of the valve prosthesis over the native aortic valve is very important for the success of the prosthesis which is explained in appendix 5.3. The current delivery systems are not steerable with more than 1 degree of freedom, causing an insufficient steerability to accurately place the valve prosthesis in a three dimensional structure, the aortic annulus.

1.2. Research Goal

The problem description above resulted in the following research question: Does an extra rotation in the distal part of the delivery system improve the ability to steer the tip to the center of the aortic annulus in a coaxial oriëntation?

Two research goals are set to answer this research question:

- Develop a prototype that provides an extra degree of freedom compared to the Edwards delivery catheter.
- Validate the functionality of the prototype with the current systems with regard to the positioning of the heart valve prosthesis.

1.3. Requirements

The final prototype of the minimally invasive delivery system has to comply with a list of requirements. It is important to keep in mind that this report will only focus on the positioning of the distal part of the prototype to answer the research question stated in section 1.2. This is the reasons why some of the listed requirements will be defined as wishes for future development of the prototype.

These requirements can be divided in 5 different dimensions of quality: performance, durability, compatibility, aesthetics and perceived quality. Performance comprises of the operating characteristics of a product and its dimension which consists out of measurable quantities; durability comprises of the life span of the product; compatibility is the state in which the delivery system and the human body are able to exist in combination without problems or conflict; aesthetics is a subjective dimension which explains how a product looks and feels; and lastly the perceived quality which is a dimension that is associated with reputation compared to current systems. Literature, anatomical boundaries and consultation with medical staff formed the basis of the following list of requirements.

Performance

- (1) The prototype cannot exceed a diameter of 6 mm [39].
- (2) The prototype has to be steerable with two rotations. Rotation A should overcome the aortic arch with a minimum rotation of 200 degrees. Rotation B with a minimum of 15 degrees (see appendix 5.2).
- (3) The prototype has to comply with the dimensions needed to perform a transfemoral aortic valve implantation. (picture with all the dimensions of the current system).
- (4) The prototype has to be used without the use of power sources other than muscle power.
- (5) The prototype should ensure a bigger range in implantation possibilities in the aortic annulus compared to the Medtronics and Edwards delivery systems.
- (6) The prototype has to be able to manoeuvre the tip of the delivery system in a coaxial oriën-tation in the aortic annulus.
- (7) The prototype has to be able to manoeuvre the tip of the delivery system in the center of the lumen of the aorta.

Durability

- (8) The catheter has to be designed to be disposable. (wish)

Compatibility

- (9) The delivery system should not cause an inflammatory or allergic reaction to the body's tissue. (wish)
- (10) The design has to cope with the wet environment of the human body. (wish)

Aesthetics

- (11) Because surgeons sometimes have to use different systems in the same hospital because of financial reasons, the prototype should have mainly similar dimensions as the current techniques and similarities in the use of the system compared to the current techniques. (wish)

Perceived quality

- (12) The delivery system should be as easy or easier to use than the current systems regarding the positioning of the tip of the delivery systems. (wish)

1.4. Thesis outline

The clinical problem together with the problem description is described above. To answer the research question that is provided by the problem description, the following steps are taken. First, the prototype has to be designed. This will be done by the reverse engineering of the Edwards delivery system. It is decided that there will be modifications to the existing Edwards delivery system. Two experiments are conducted to provide the best configuration for the modification to the Edwards system. The findings in the reverse engineering of the Edwards delivery system and the results of the experiments are combined to provide a prototype that satisfies the list of requirements. Subsequently, the prototype will be validated in the final experiment in chapter 3. Lastly, the validation and the design of the prototype will be discussed from clinical perspective and recommendations are given for future research and development.

2

Method

To achieve the goals that were set in the previous chapter, different steps were taken to design the prototype that will answer the research question. This chapter will focus on the designing of the prototype. The method for the design is started with the reverse engineering of the Edwards DS to give insight in the mechanisms that are used. Subsequently, these mechanisms are modified to the needs of the prototype, stated in the list of requirements. Two experiments are performed to substantiate the choices for the modification in the prototype. Lastly, the final design of the prototype will be described.

2.1. Reverse Engineering

To get a clear image on the current technique that is already steerable with 1 rotation, the Edwards system is disassembled to have a closer look at the mechanisms that are used to provide rotation of the tip. The DS is visible in figure 2.1 and all the different components are marked in different colors. The handle and the outer catheter are the focus points of this research because these contain the techniques that provide the rotation.

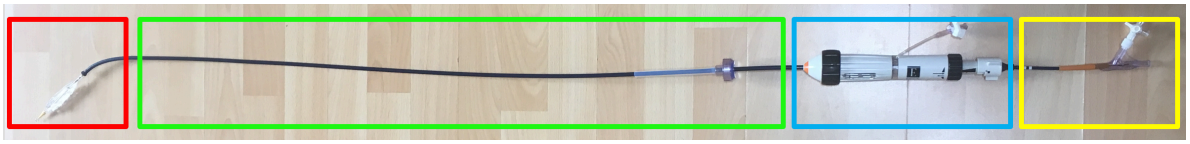

Figure 2.1: Edwards delivery system with the inflatable balloon on the distal end of the DS(Red) the outer catheter (Green), the handle (Blue) and the inner catheter (Yellow). The inner catheter is connected to the inflatable balloon and runs through the handle and outer catheter.

The handle consists out of two parts that are visible in part C of figure 2.2. The proximal part is visible on the left hand side of section C and the distal part is visible on the right hand side of section C. The distal part of the handle is used to control the rotation of the tip of the delivery system. The proximal part of the handle is used to control the depth of the inner catheter relative to the outer catheter.

First, the mechanism for tip deflection is explained and the mechanism is visible in section B. These parts are normally placed inside the distal part of the handle. Part J is normally placed over the rails, visible at the lower part of section C. Part J has a screw thread on the outside, but it also has a screw thread on the inside. The white knob, called part K, is placed on the rails and moves in a linear line over the rails, as is displayed by the red arrows. Part K is moved through the inside of part J when part J is rotated. This movement is created by rotating wheel E which ensures a rotation of part J and subsequently the movement up or down the rails of part K, dependent on the rotation clockwise or counterclockwise of wheel E. The metal wire that is depicted in section A of figure 2.2 runs through a duct on the inside of the outer catheter. One end of the metal wire is connected to the above mentioned part K visible in section B that can move over the rail. The other end of the metal wire is connected to the distal part of the outer catheter.

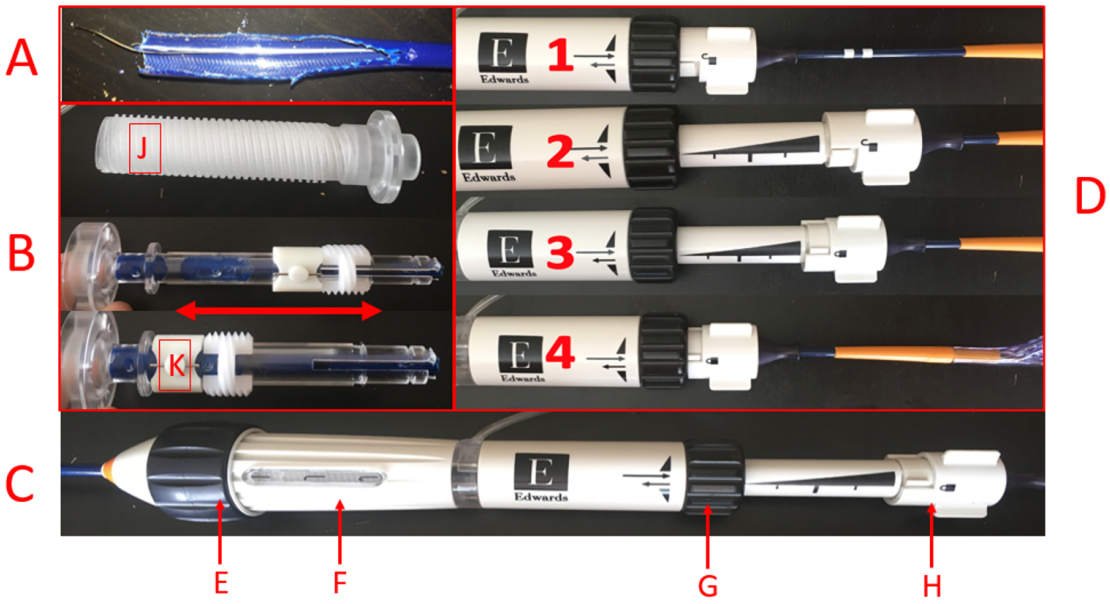

Figure 2.2: The steel cable that runs through the outer catheter is depicted in section A. The mechanisms for tip deflection is depicted in section B. The handle of the Edwards catheter(C) with the rotation wheel for deflection (E); the flex indicator (F); the rotation wheel for depth control of the inner catheter (G); and a lock and release knob for fixation and release of the inner catheter (H). Lastly, the steps for the control of the depth of the inner catheter relative to the outer catheter is shown in section D.

Summarizing, wheel E ensures a rotation of part J, which ensures a translation of part K in section B that subsequently puts tension on the metal wire. This tension force, that is exerted on the distal part of the outer catheter, causes the tip to rotate. Lastly, the flex indicator at point F gives the user an indication on the amount of rotation of the distal part of the catheter.

The mechanism for the depth control of the inner catheter and the balloon relatively to the outer catheter will be explained and is visible in section D of figure 2.2. The movement is created by rotation wheel G and the lock and release knob H in section C. The steps for the movement of the inner catheter are displayed in section D of figure 2.2. During step 1, knob H is unlocked and the handle can be translated over the inner catheter without moving the inner catheter by wheel G. When knob H has arrived in a more proximal position, depicted at step 2 in section D, the knob can be rotated ensuring a lock to the inner catheter displayed at step 3. Lastly, the inner catheter, that is locked to knob H, can be moved to a more distal position relative to the outer catheter by rotating wheel G counterclockwise. These steps can be repeated or reversed which causes movement of the inner catheter relative to the outer catheter.

The distal tip of the outer catheter has a structure that is displayed in figure 2.5 in which the folded heart valve prosthesis, that is visible in figure 2.3, can be placed. The placement of the prosthesis in the structure of the tip of the outer catheter ensures that the prosthesis moves in the direction that the tip is pointing. The outer catheter has a length of 1050 mm and in 100 mm of the distal part of the outer catheter a metal casing with laser cuts is placed in the wall of the catheter. This ensures that the distal part of the catheter doesn't fold when it is bend in an angle.

The inner catheter has two different functions. First, the inner catheter in combination with the handle mechanism, that is explained above, gives controllability of the implantation depth of the heart valve prosthesis. Moreover, the inner catheter serves as a duct for the fluid that is used to inflate the balloon during balloon valvuloplasty to unfold and anchor the heart valve prosthesis in the aortic annulus.

The inner catheter with the balloon mounted on the tip can move in a straight line up and down in the angle of the outer catheter that is set with rotation wheel E. Inflating the balloon slightly will ensure a connection of the prosthesis to the balloon by friction between the prosthesis and the balloon. The movement of the inner catheter relative to the outer catheter with the prosthesis connected to the balloon, provides control over the implantation depth of the heart valve prosthesis in the aortic

annulus.

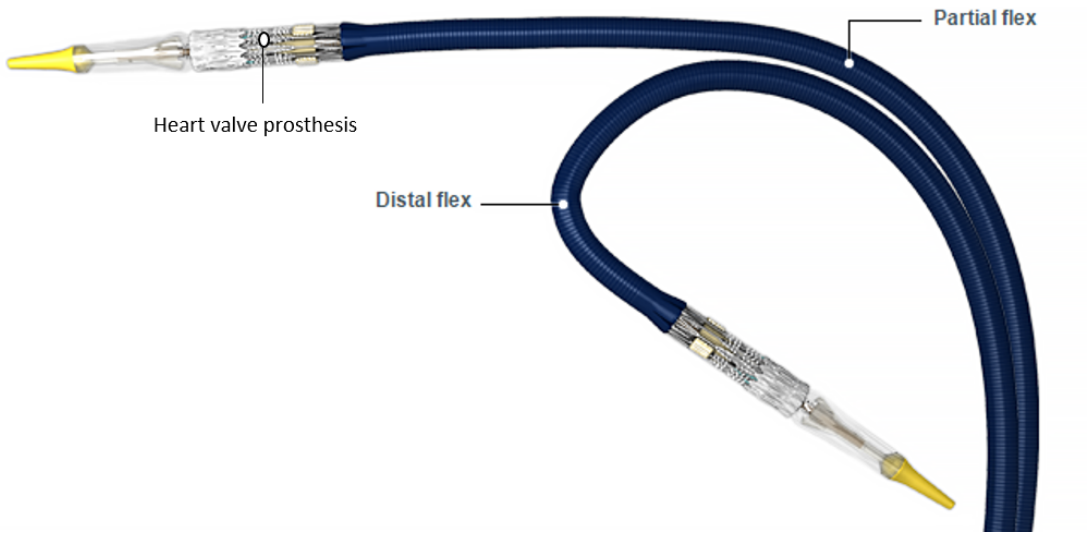

Figure 2.3: The distal part of the Edwards DS with the folded heart valve prosthesis, showing the rotation of the distal tip of the DS.

Conclusion

The focus of the research question is on the positioning of the heart valve prostheses, hence the interest in the steering mechanism in the outer catheter and handle explained in the previous chapter. The mechanism for the rotation of the distal tip of the Edwards DS is a proven concept. Not only does this mechanism satisfy the requirements for the performance, but it also satisfies the requirement to make it easy and recognizable for the user, which is the surgeon.

The backwards engineering of the handle and the catheter showed the different mechanisms that ensure the delivery and positioning of the heart valve prosthesis. Combining the outer catheter with the distal part of the handle in figure 2.2, provides the steerable degree of freedom of the Edwards catheter. The inner catheter in combination with the proximal part of the handle in section C of figure 2.2 controls the depth of the balloon and subsequently the prosthesis when the outer catheter is placed in the correct angle.

Figure 2.4: Isolated part from the Edwards catheter with the steerable technique isolated. This part is used for further development of the prototype.

Future steps after the reverse engineered Edwards DS

To design a prototype that provides the extra degree of freedom in the form of an extra rotation, described in chapter 1, these parts have to be modified to the needs stated in the list of requirements. The Edwards DS is disassembled until the mechanism for the rotation of the delivery system is isolated, this is visible in figure 2.4. This part will ensure rotation A, which is described in chapter 1. The proximal part of the handle, visible in section C of figure 2.2 and the inner catheter are removed, because this mechanism doesn't aid in the steer ability of the distal tip of the DS and will not be needed within the scope of this research. The removal of this mechanism opens possibilities to adjust the existing

delivery system.

A discussion between the author and the instrument maker led to the conclusion that the inner catheter can be replaced with the material Poly(ether-ether-ketone) (PEEK) which is cheap and easy to modify. The PEEK has to be modified to the needs that are specified in the list of requirements and that is why an experiment is needed to explore the effects of modifications on PEEK.

Figure 2.5: The tip of the Edwards delivery system in which the stent is placed to provide support

2.2. Effects of notch configuration on PEEK specimens

Introduction

To explore the effects of modifications to catheter strip that are made from Polyether-ether-ketone (PEEK), an experiment is conducted. Insight in the effect of different modifications to the PEEK catheter strips will help to choose the correct configuration for the application in the prototype of the delivery system. PEEK strips will be modified by adding notches on two sides of round PEEK strips, 180 degrees apart from each other which is visible in figure 2.6.

A pulling wire (PW) is attached to the tip of the catheter. When tension is put on the wire, the catheter tip starts to rotate in the directions of the red lines that are visible in figure 2.7. The independent variables that can be manipulated for this experiment are (1) the amount of notches over a distance of 20 mm of 40 mm PEEK strips, (2) the width of the body between the notches and (3) the diameter of the PEEK strips. The three independent variables result in a total of 8 experimental conditions (EC). The goal of this experiment is to analyze the effects of these independent variables on the dependent variables which are in this case the force in the pulling wire and the angle of rotation of the catheter specimens in degrees.

Material

The material that will be used for the catheter speciemens is Polyether-ether-ketone which is cheap and easy to modify. It has a very good mechanical property spectrum with a modulus in the range (3 to 150)GN m^{-2} at 23°C and strength in the range (100 to 2,000)MN m^{-2} at 23°C [17]. Two sizes will be used for this experiment: 1.8 mm outer diameter and 2.0 mm outer diameter. These will be cut into strips of 40 mm of which 20 mm will be used to mill notches of 0.3 mm wide. The notches will be milled 180 degrees apart from each other with configurations given in table 2.1. The milling of the notches will give more flexibility in the directions given in figure 2.7.

Experimental Condition (EC) (EC)	Outer Diameter PEEK [mm]	Amount of notches [n]	Width of body between notches [mm]
1	2.0	20	0.6
2	1.8	20	0.2
3	2.0	10	0.3
4	1.8	10	0.5
5	1.8	10	0.2
6	2.0	10	0.6
7	1.8	20	0.5
8	2.0	20	0.3

Table 2.1: Configuration of the notches in the PEEK specimens applied over a length of 20 mm of the material.

Equipment

For this experiment a linear stage is used to provide the movement needed to put tension on the wire that will deflect the tip of the catheter. A clamping holder is fabricated to clamp the catheter specimens in a vertical configuration, see figure 2.6. Moreover, a 9 Newton FUTEK load cell is placed between the linear stage and the tension wire of the specimen to measure the increase of force during the linear movement of the stage and consequently increase of the tension in the pulling wire. This load cell is connected to a Labjack UE9 Series with a 0-5 Volt Maximum Analog Input Range. The software Matlab 2015b is used on an Apple Macbook Pro to process the data.

Method

The following steps are performed to conduct this experiment. First, the specimen is put in the clamping holder and clamped with the body between the notches in the middle and the notches pointing to each side, see figure 2.7. Behind the specimens there is a protractor to measure the angle the specimen makes when it is rotating. The pulling wire is attached to the load cell that is connected to the linear stage. The starting point is set for the linear stage as the point where the wire under tension. In this phase, the setup is ready for the run and the movement of the linear stage is initiated with Matlab with

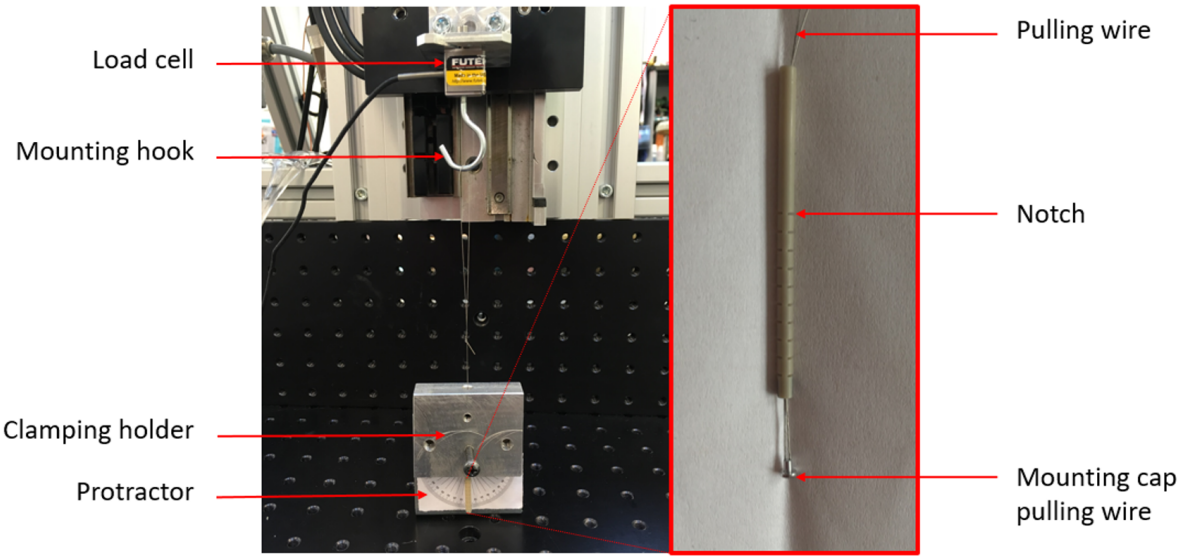

Figure 2.6: Experimental setup with all the equipment depicted on the left and an enlarged view of the catheter specimen on the right.

a speed of 0.1mm/s for a distance of 2mm, together with the starting of the camera to record the run. When the run is completed, the linear stage will move back to the starting position, the video recorder will be stopped and the catheter specimen will be changed for the next specimen. The experiment is conducted 5 times on each specimen in random order to reduce bias, making a total of 40 runs. The randomization was performed by the function "Rand" in the software Matlab. The raw data was processed in Matlab with a moving average filter with kernel size 20 to reduce the amount of noise in the data and the raw data was multiplied with a factor 0.85 to convert the data from Volt to Newton. After the all the experiments are completed, the video of each run is inspected and the deflection in degrees, read from the protractor behind the the PEEK specimen, is noted.

Results

When the experiment was conducted, it showed that there was no rotation of the tip of the specimen in EC6, but this was still considered as a result, hence a total amount of runs of 40 which were included in the experiment.

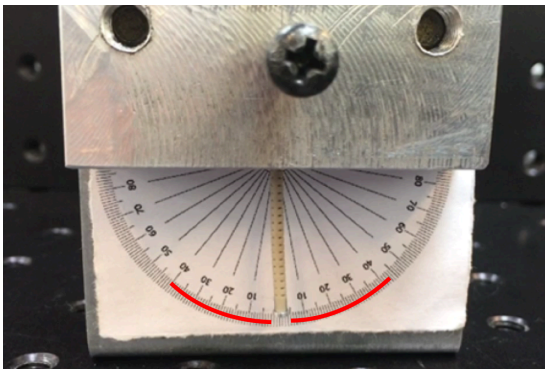

Figure 2.7: The route the tip will travel during rotation is visualized by the red lines.

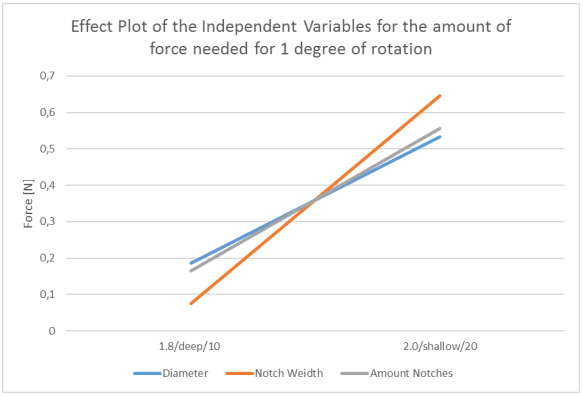

Figure 2.8: Effects plot of the independent variables on the dependent variable force in Newton that is needed for 1 degree of rotation.

Figure 2.9 shows the amount of rotation in degrees of the specimen per 1 Newton of tension. It shows that the EC 1, 4, 6 and 7 are the experimental conditions with the lowest deflection per Newton

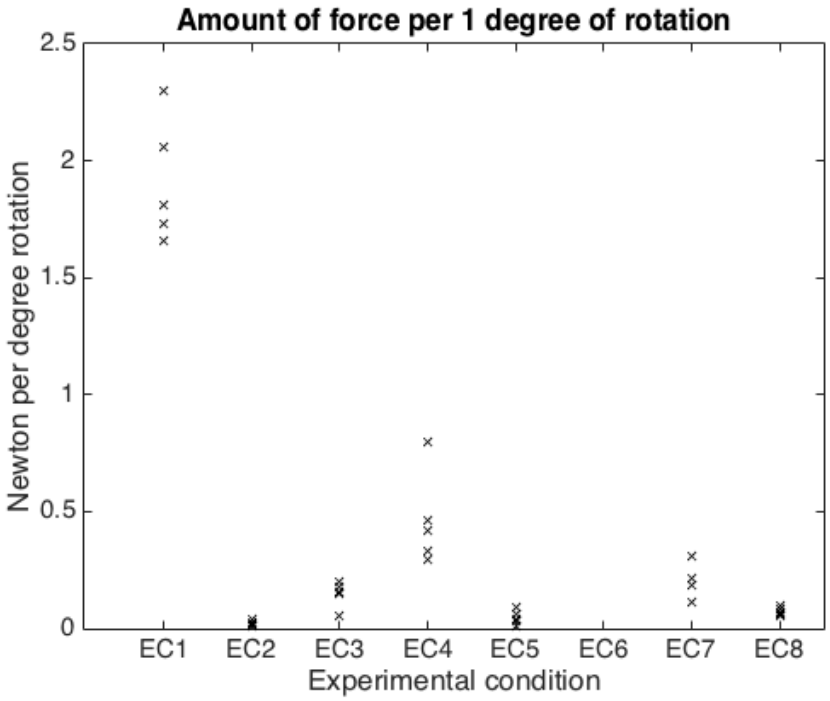

Figure 2.9: The amount of rotation in degrees per Newton of tension in the tension wire of the catheter specimen.

tension. These are the conditions with the biggest body between the notches. Moreover, EC 2 and 5 are the experimental conditions with the lowest width of the body between the notches, 0.2 mm, and resulted in the highest deflection per Newton tension in the wire. In comparison, the specimens with the lowest deflection per Newton tension, are the specimens with the highest width of body between the notches, 0.6 mm.

If we look at the effects plot, which displays the means for each group within each experimental condition, we see what kind of effect the independent variable has on the dependent variable. The effects plot of the experiment in figure 2.8 for the independent variables shows that the biggest effect is realized with the width of the body between the notches. Moreover, the ANOVA shows that the means are significantly different with p-values for respectively the diameter, body width and amount of notches of 0.0345, 0.0009, 0.0182. This also shows that the effect of the notch width has the lowest p-value indicating the biggest difference in means for both states within the independent variable.

Discussion/Conclusion

Eight different experimental conditions were created by modifying catheter strips that were made from the material PEEK. The specimens were placed under a linear stage and a tension wire, that was connected tot the tip of the specimen, was connected to the linear stage. When tension was applied to the wire by the movement of the linear stage with a speed of 0.1mm/s, the tip of the PEEK started to rotate. Video footage of the runs was used to read the maximal amount of rotation in degrees by a degree bow behind the specimen. Moreover the amount of force on the tension wire was measured during the run. Knowledge of the deflection and the amount of force needed for the deflection for every EC will help in the selection of the best configuration needed for the prototype.

The effect plot shows that the biggest effect on the amount of force needed for rotation is achieved with the variation in width of the body between the notches. This can be explained by visualizing that the body between the notches is the area around which the specimen will rotate. The bigger this area is, the more resistance it will provide against the rotation.

Another interesting observation was that the variance in the amount of rotation was high for the experimental conditions: 2, 3, 5, 7 and 8 (respectively 133.3, 34.5, 238.2, 54.7 and 134.8). This could be explained by the technique in which the tip was deflected. The specimens were produced with two

tensions wires connected to the tip for a deflection to either side of the specimen. These wires could have been rotated around each other in the catheter strip, resulting in a tension that is not exerted on the outside of the specimen. This causes the force to be more to the center of the specimen which could result in a smaller rotation compared to other runs in the same EC. Moreover, the two tension wires were connected to a cap that was put on the tip of the specimen, but this cap could rotate because it was not firmly fixated to the specimen. The rotation of the cap also results in a force that is more exerted on the center of the catheter specimen which results in a smaller deflection. So the rotation of the wires around each other and the cap relatively to the catheter specimen could be an explanation for the high variance of the deflection per Newton within the experimental conditions.

A limitation of this experiment is the small amount of runs per experimental condition. The results show an effect, but the variance for the rotation is high within the experimental conditions. For further research the amount of independent variables have to be scaled down so more runs can be performed per EC, increasing the statistical power.

In conclusion, this experimental setup gave insight in the behaviour of modifications to the catheter strips. Both the diameter as the body width and the amount of notches caused an effect on the amount of force needed for 1 degree of deflection of the catheter specimens, but the biggest effect was found in the variation of body width of the catheter strips. Further research is needed to select the best configuration for the prototype. Recommendations for further research are to focus on one independent variable: the body between the notches. Furthermore, a recommendation is to increase the amount of runs per experimental condition to improve the statistical power. Lastly, modifications to the catheter strips have to be performed to remove the effect of the twisting of the pulling wire around each other. In addition the rotation of the cap in the catheter to which the pulling wire is attached has to be prevented.

2.3. Selection of PEEK specimen after variation of body width

Introduction

To satisfy the list of requirements stated in the introduction of this report the best configuration of the PEEK catheter strip, that is going to be a modification to the current Edwards catheter, has to be selected. The list of requirements shows that a rotation of 15 degrees has to be provided to satisfy the needs of the prototype. The pulling wire of the modification will run through the outer catheter to the handle. The handle will control the amount of force exerted on the modification. The amount of force needed for this rotation has to be as low as possible, because it would otherwise affect the shape of the outer catheter. The configuration that provides a rotation of 15 degrees with the least amount of force is preferable. This results in the research question: What configuration of the catheter specimen will create a rotation of 15 degrees with the least amount of force needed for the rotation?

To answer this question a follow up study of experiment 1A is conducted. The independent variable in this experiment will be the size of the body between the notches and the dependent variables will be the angle of rotation of the tip of the catheter and the force in the pulling wire. The force in the pulling wire will be created by the movement of a linear stage.

The experiment in chapter 2.2 concluded that the biggest effect is realized with variation of the body between the notches. Moreover, the recommendation were to modify the catheter strips, reduce the amount of ECs and increase the amount of runs per EC. These recommendations are taken into account in this experiment and the results of this experiment will provide a clear recommendation for the selection of the modification for the prototype.

Material

The modification will be placed on the tip of the isolated part of the Edwards catheter that is visible in figure 2.4. The inner diameter of this outer catheter is 3mm. Therefore, PEEK catheter specimens with an outer diameter of 3.1 mm will be used for this experiment, so that a tight fit can be achieved when it will be mounted to the isolated part.

Moreover, the catheter strips are adjusted to overcome the problems with the tension wires that were experienced in the previous experiment. The pulling wire is still attached to a cap that is placed in the tip of the catheter, but for this experiment there is only 1 pulling wire attached to this cap to resolve the problem of tangled pulling wires. Additionally, the cap is glued to the tip of the catheter tips to prevent the cap from rotating relatively to the catheter specimen.

The notch width was determined by calculating the ratio between the diameter of the catheter and the body between the notches in the previous experiment. This resulted in a configuration with a body of 0.35 mm for the smallest configuration. If we calculated the ratio for the highest body between the notches, this gave a configuration of 0.95 mm. Because this configuration resulted in no rotation in the previous experiment, so a smaller body is chosen. Ultimately, four PEEK catheter specimens with an outer diameter of 3.1 mm are tested with the configurations of the notches given in table 2.2. On each specimen 20 notches are evenly divided over 20 mm opposite to each other, resulting in a distance between the notches of 2 mm.

Experimental Condition (EC) (EC)	Outer Diameter PEEK [mm]	Width of body between notches [n]
1	3.1	0.35
2	3.1	0.50
3	3.1	0.65
4	3.1	0.80

Table 2.2: Experimental conditions with the configuration of the notches in the PEEK specimens.

Equipment

Also for this experiment a linear stage is used to provide the movement needed to put tension on the wire that will deflect the tip of the catheter. The same clamping holder is fabricated to clamp the catheter specimens in a vertical configuration, see figure 2.6. For this experiment a 22 Newton FUTEK load cell is placed between the linear stage and the PW of the specimen to measure the increase of force during the linear movement of the stage and consequently increase of the tension in the pulling wire. This load cell is connected to a Labjack UE9 Series with a 0-5 Volt Maximum Analog Input Range.

The software Matlab 2015b is used to process the raw data.

Method

The same method as in experiment 2.2 is used for this experiment, the description is visible in chapter 2.2. The modification in the method compared to the method in experiment 2.2 is a factor of 2.355 for the conversion of the output in Volt to the force in Newton and the amount of runs. There are a total of 4 ECs and every EC is tested 15 times. To add validity and to provide protection against systematic influence of uncontrolled variables, the experimental runs are randomized with the function ”rand” in Matlab.

Results

All the 60 runs were successfully completed and are taken in consideration in the results. The summarizing plots are visible in figure 2.10 and 2.11.

Figure 2.10 shows the amount of force that's needed for 1 degree of rotation of the tip of the specimen. It shows that in increase in body between the notches results in an increase in force that's needed to rotate the tip. Moreover, it shows that the variance decreased a lot compared to experiment 1A with values for increasing body between the notches of respectively $6.1454e^{-05}$, $2.1936e^{-04}$, $2.6732e^{-04}$ and $3.3604e^{-04}$. In figure 2.11 a boxplot is displayed for the dependent variable, force per degree of rotation, per EC.

Besides the amount of force that was measured per EC, the angle of rotation for the different ECs are determined. It showed that a pulling distance of 2.5 mm resulted in a rotation of the tip of the catheter of 20 degrees in EC2. For EC1 there was a rotation of 30 degrees and EC3 and EC4 didn't manage a rotation of 15 degrees with a pulling distance of the linear stage of 2.5 mm.

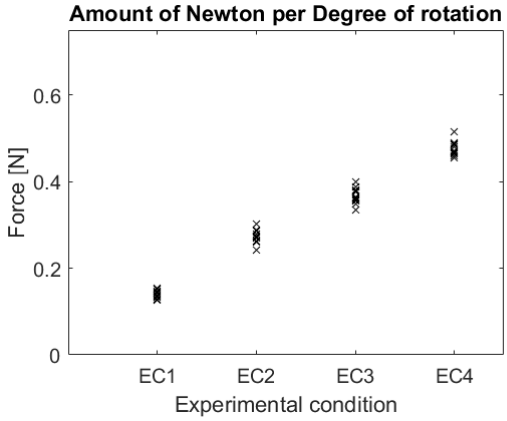

Figure 2.10: The amount of rotation in degrees per Newton of tension in the PW of the catheter specimen.

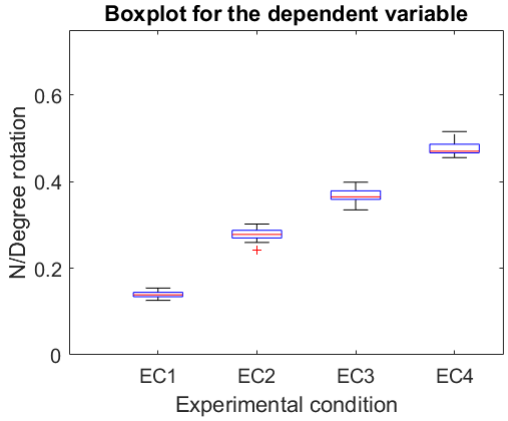

Figure 2.11: Boxplot of the dependent variable per EC.

Discussion/Conclusion

Four different experimental conditions were created for this experiment by modifying catheter strips that were made from the material PEEK. This was a follow up study on experiment 2.2 were there were some imperfections in the experimental setup and inconclusive results. Modification to the catheter strips and the amount of runs resulted in a clear image to answer the question: ”What configuration of the catheter specimen will create a rotation of 15 degrees with the least amount of force needed for the rotation?”. Combining the results of the dependent variables force and angle on the independent variable notch body width can answer this question.

It showed that EC2 can manage a rotation of 20 degrees with a force of 0.6 Newton. EC3 and EC4 couldn't manage a rotation of 15 degrees when the pulling wire was pulled for a distance of 2.5 mm. Furthermore, there is a higher force needed to rotate the tip of the catheter 15 degrees than in EC2. EC1 showed a rotation of 30 degrees which is double the amount of the rotation that is needed for the prototype.

In conclusion, the results showed that EC2 with a body width between the notches of 0.5 mm gave

the possibility to rotate the tip of the catheter tip at least 15 degrees when the PW was pulled for a distance of 2.5 mm. From these results is concluded that this configuration that is going to be used for the prototype will be a PEEK catheter strip with a outer diameter of 3.1 mm modified with a total amount of 20 notches, 10 on either side, with a width between the notches of 0.5 mm.

2.4. Final Concept

The mechanism for the handle and the modification of the tip are discussed in the previous chapter. The tip that is selected from experiment 2.3 is added to the isolated part from the Edwards delivery system depicted in figure 2.4. Moreover, the handle is modified so that the second rotation, referred to as rotation B in figure 1.5, can be controlled. The prototype is visible in figure 2.4 and the two sections that are modified are depicted in section A and B. Section A displays the tip of the prototype and sections B shows the handle. This chapter will elaborate on the mechanisms of these parts and the specifications.

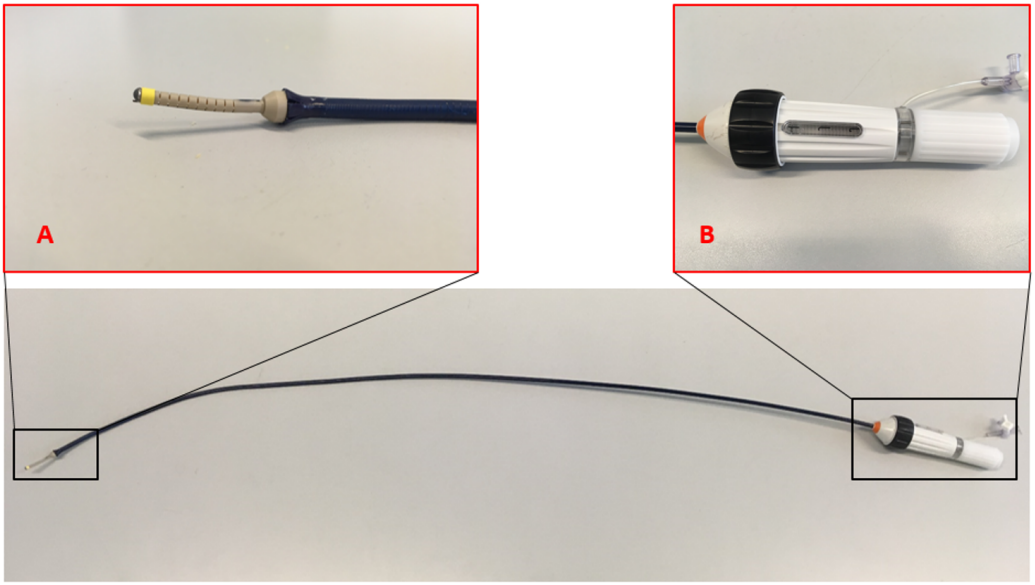

Figure 2.12: The prototype with an enlarged image of the tip of the prototype depicted in A and the handle depicted in B.

2.4.1. Handle

The mechanism of the handle is based on the the proven concept of the Edwards delivery system that is disassembled in chapter 2.1. The part of the handle that controls rotation A is kept the same and is explained in chapter 2.1. The modification on the handle is depicted in section 1 of figure 2.13. Part A and B move over the rails in the directions indicated by the green arrows. The metal pulling wire that runs through the handle and catheter to the tip is connected to part B. The handle that is visible in section 3 has a screw thread on the inside of the handle indicated at the green arrow. This part is placed over the rails with part A and B and locked with a clip indicated in section 2 by the green arrow. The rotation of the handle clockwise or counterclockwise ensures movement of part A in section 1. A rotation counterclockwise will ensure a movement of part A to the distal part of the handle. This causes tension in the pulling wire that is connected to the modification in the tip and this tension will cause a rotation of the tip. When the tension is released by rotating the handle clockwise, resulting in a movement of part A to the left in section 1, the tip will straighten out by the elastic properties of the material of the modification at the tip. The amount of movement of part B in section 1 of figure 2.13 is 32 mm and a rotation of 1040 degrees is needed to get maximum rotation of the tip.

2.4.2. Catheter

The catheter tip that is made from the material PEEK is displayed in section A in figure 2.4. The configuration selected in chapter 2.3 is chosen for this modification resulting in a tip with a width of 3.1 mm with a notch configuration of 20 notches evenly spread with a body between the notches of 0.5 mm. The catheter strip is pressed into a base with a diameter of 4 mm. This base is glued into the tip of the isolated part depicted in figure 2.4 to provide a strong connection. A similar cap as in figure 2.6 is placed inside the tip of the modification with 1 steel pulling wire. The pulling wire runs trough the inside of the catheter to the handle and is connected to part B in figure 2.13. The modification of

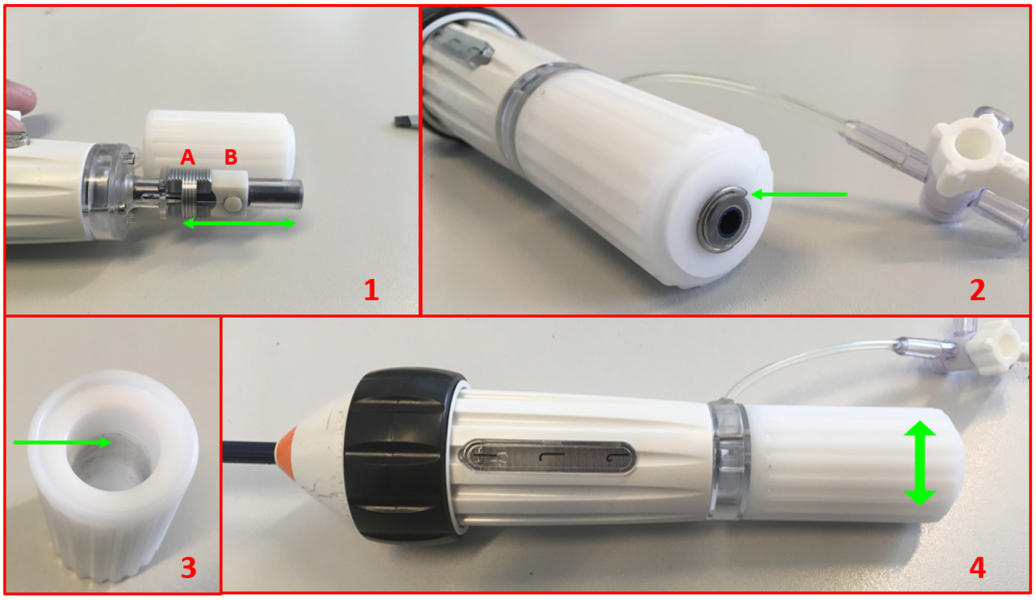

Figure 2.13

the tip has a length of 35 mm and the maximum width is 6 mm at the point where the modification is connected to the outer catheter.

3

Validation

3.1. Introduction

To answer the research question, "Does an extra rotation in the distal part of the delivery system improve the ability to steer the top to the center of the aortic annulus in a coaxial oriëntation?", a validation study is performed. The focus of this experiment will be on the positioning of the tip of the delivery system in a glass phantom model of the aorta. An Aurora system will track the position of the tip of the delivery systems in a 3D environment. The Medtronics delivery system, which is not steerable, the Edwards delivery system, which is steerable with 1 rotation and the prototype that is steerable with 2 rotations will be compared in this study.

A total of two technical tests are performed and one user test. First, a technical test is performed where the reach and possible angle oriëntations of the three different systems in the aortic annulus will be compared. Moreover, the ability of the three systems to be steered to a reference point that reflects the center of the aorta lumen coaxial to the ascending aorta. The third test is a user test where thorax surgeons will execute the technical test for feedback on the handling of the delivery system. To answer the research question, the results of the two tests will be discussed to determine whether the prototype is better in the positioning than the current techniques.

3.2. Materials

3.2.1. Test specimens

Three different delivery systems are used for this experiment: The Edwards delivery system; The Medtronic delivery system; and the prototype that is developed in chapter 2. The Medtronics delivery system is not steerable but allows 1 rotation in direction A, depicted in figure 1.5. By pushing the system upwards, the tip will be deflected by the resistance of the artery wall. The Edwards delivery system is steerable with 1 rotation to align the tip in the frontal plane to the aortic annulus, depicted in figure 1.5 as rotation A. Lastly, the prototype will provide the same steerable rotation as the Edwards catheter but is also steerable with a rotation in the sagittal plane, depicted in figure 1.5 as rotation B.

3.2.2. Equipment

The setup for this experiment, depicted in figure 3.2, consists of the glass aorta model and two stands that hold the glass model in position. The stands are taped to the table with double sided tape to ensure that the model doesn't move during the experiment. The phantom model is made from glass with the dimension described in Appendix 5.2.

The position of the tip of the delivery systems is important for the positioning in the aortic valve, hence the use of an Aurora NDI system to track the position of the tip of the delivery system. Each delivery system is equipped with an Aurora 5DOF Sensor 0.5 mm x 8 mm that gives information about 5 degrees of freedom in a three dimensional space: xyz-coordinates and the rotation around the x- and y-axis.

To define the point which represents the center of the aortic annulus and coaxial to the ascending aorta of the model, a cap that perfectly fits on the aortic phantom model is 3D printed. In this cap

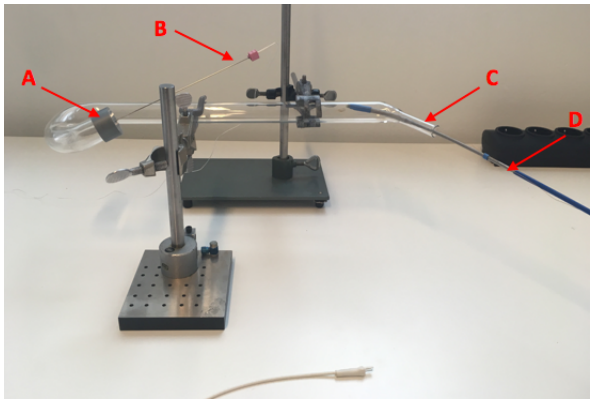

Figure 3.1: The setup of this experiment, where the cap for the definition of the end position is visible at point A, the chiba-tip needle at point B, the entry of the aorta model at point C and the delivery system at point D.

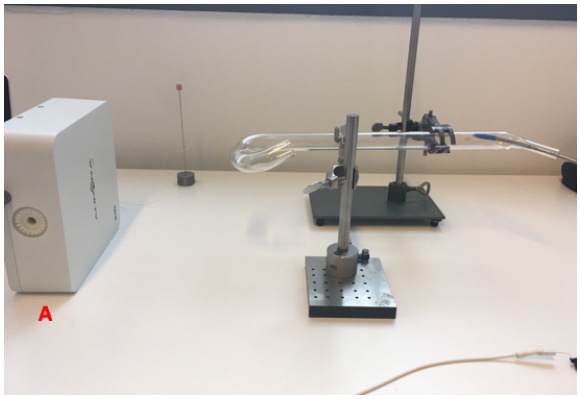

Figure 3.2: The Aurora system that creates a magnetic field to track the sensors in a 3D environment is visible at point A. The delivery system enters at the right and is manoeuvred to the other side of the glass model to position the tip in the aortic valve.

a 5 mm deep hole with a diameter of 1.2 mm is drilled so that a Chiba-tip needle with a diameter of 1.2 mm perfectly fits in this hole. This cap in combination with the chiba tip needle ensures a coaxial oriëntation of the needle in the center of the aortic annulus. In figure 3.1 this combination is visible at point A and B and is used to define the reference point for the user to manoeuvre the tip of the distal part of the delivery systems towards.

Data acquisition and the control of the Aurora system are achieved using the provided Aurora Toolbox "Track" on an Apple Macbook Pro. The recording of the data can be initiated and ended with this software. The sampling frequency of the Aurora system is 50Hz. The following variables for the sensor on the delivery system and the reference point were stored on the computer: (1) coördinates on the x-, y- and z-axis; (2) the rotation around the x- and y-axis.

3.2.3. Users

The technical tests used for the data acquisition will be done by the author. Moreover, two thorax surgeons will use the three systems in the experimental setup for a user test. Their feedback on the handling of the prototype in comparison with the current techniques will be discussed.

3.3. Method

3.3.1. Procedure

After setting up the equipment stated above in the arrangement depicted in figure 3.2, the experimental runs were performed by the author. There were always two persons present, the user to perform the runs with the delivery systems and a helper to start and stop the runs in the toolbox for the Aurora system on the Macbook Pro.

Two tests will be performed in this experiment to validate the functionality of the prototype in comparison to the existing delivery systems. First, the reach of each delivery system in the aortic annulus of the model is determined. Second, the ability in which the tip of the delivery system can be steered to the reference point is determined by measuring the error in position and rotation.

Technical test 1

The position of the wall of the aorta lumen will be determined by moving the tip of the chiba tip needle sensor in a helical movement up and down the wall of the ascending aorta of the glass model. The boundaries of the inside of the glass model are acquired in a three dimensional space by this movement. Hereafter, three runs will be performed the three delivery systems will be maneuvered to the ascending aorta and moved around in all the possible positions the delivery system will permit. The Medtronics delivery system can only be pushed upwards and downwards into the glass model. The Edwards delivery system has three options for manipulation. (1) It can be pushed upwards and pulled back into the aorta. (2) The tip can be rotated with the flex wheel E, depicted in figure 2.2. (3) Lastly,

the handle of the Edwards delivery system can be rotated to produce torque in the outer catheter. The rotation of the handle will be done for a maximum of 180 degrees in each direction. The same options account for the prototype, but in addition this delivery system has an extra rotation resulting in rotation B in figure 1.5 of the tip. The amount of rotation is controlled by an extra flex wheel, depicted in figure 2.13.

Technical test 2

The experimental runs will be performed 5 times with each delivery system resulting in a total amount of runs of 15. To lower the time between runs and to lower the chance of malfunctioning of the sensors because of the need to change the connections to the Aurora system, the run for every delivery system is repeated 5 times, starting with the Medtronics delivery system, followed by the Edwards delivery system and ending with the prototype. Manipulation of the delivery system is only allowed on the proximal end of the delivery system.

The protocol for a single experimental run was the following:

1. (1) Set up the experiment as is depicted in figure 3.1
2. (2) Put the delivery system at the entry point of the glass model, visible at the right side of figure 3.1
3. (3) Set the name for the specific run in the software and select the two sensors that have to be recorded.
4. (4) Start the recording of the data.
5. (5) After a minimum of 100 samples are taken, remove the cap with the needle depicted at point A and B in figure 3.1.
6. (6) Let the user start maneuvering the tip of the delivery system in a coaxial position in the center of the aortic annulus and tell him to say ”stop” when he thinks the perfect end-position is reached and stop the recording of the data.
7. (7) Remove the delivery system from the glass model.

User Test

The user test will use the same procedure as technical test 2, but the surgeons will only perform the runs once for each delivery system. In this way they can compare the handling of the three delivery systems to each other.

3.3.2. Data processing

Technical test 1

The data set acquired from this test is used to determine the reach of all the three delivery systems within the aorta lumen. To visualize the position of the tip of the DS, the The traveled pathway is plotted together with the rotations around the x- and y-axis.

Technical test 2

The data set obtained from this experiments consist of time histories of positions and angles of two sensors in a three dimensional space. The points of interest of this dataset are the first data samples of the chiba tip needle sensor that is visible at point B in figure 3.1 and the last data samples of the sensor that is mounted to the tip of the delivery system.

The accuracy error of the Aurora system is stated as 0.7 mm in Aurora user guide. To filter this error, the average over 100 samples is used for the chiba tip needle sensor that represents the reference point. The average over the last 20 samples is used from the sensor data from the tip of the delivery system to define the end-position.

The two points of interest are examined and the position of the chiba tip needle is taken as reference point. To examine the position of the tip of the delivery system with regards to the reference point, the xyz-coordinates of the reference point are subtracted from the xyz-coordinates of the sensor on the tip of the delivery system, giving the error of the position of the tip in every axis relatively to the reference

point. This error (SE) in the distance from the sensor on the delivery system to the reference point is calculated using formula 3.1 where X, Y and Z are the coordinates on every axis.

$$SE = \sqrt{(X_{instrument} - X_{reference})^2 + (Y_{instrument} - Y_{reference})^2 + (Z_{instrument} - Z_{reference})^2} \quad (3.1)$$

Moreover, the error in the angle on the X an Y axis is determined by subtracting the angle of the reference from the angle of the tip of the delivery system. The results will be elaborated in the following chapter.

3.4. Results

3.4.1. Technical test 1

The experimental run for every DS is plotted in figures 3.3. The figures show the wall of the glass aorta model that is constructed by the helical movement of the chiba-tip needle sensor in red. In addition, the pathway of the delivery systems are plotted in blue. It is important to visualize that the view is from inside the ascending aorta looking to the aortic annulus. It is clearly visible that the Medtronics DS, which is not steerable, can only remain on one side of the aortic model. The Edwards DS, which is steerable with one rotation can be steered to the inside of the aortic lumen, as the second plot in figure 3.3 clearly shows. Lastly, the prototype which is steerable with two rotations, has a reach that covers most of the lumen of the aorta.

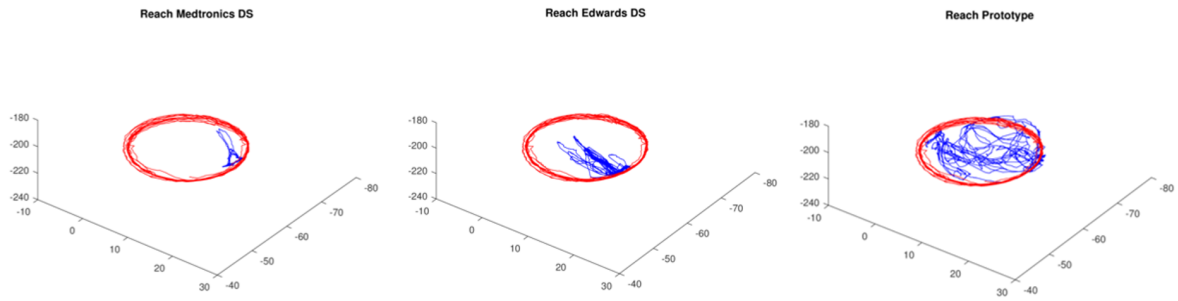

Figure 3.3: Illustrating the reach of the three delivery systems in blue within the aorta lumen. The aorta wall is depicted in red and the blue lines illustrate the position of the tip of the delivery system over time. The view is from within the ascending aorta to the aortic annulus.

Besides the reach in xyz-coordinates, the rotation around the X- and Y-axis are acquired during the runs. In figure 3.4 the rotation around the x-axis is plotted over time. This is the rotation is depicted in figure 1.5 as rotation A. In this figure only the data of the Edwards DS and the prototype are plotted because these delivery systems are steerable in this plane. It shows that the prototype has a bigger reach concerning the angles which it can achieve within the constraints of the glass aortic model compared to the Edwards delivery system.

The rotation around the X- and Y-axis was determined for the ascending aorta of the model by aligning the chiba-tip needle with the glass aorta model. It indicated a rotation of 17.7 degrees on the Y-axis and a rotation of 21.9 degrees on the X-axis. It is important to keep this in mind for the following result.

The rotation around the Y-axis is visible in figure 3.5 for the tip of each of the delivery systems. This plot represents the sagittal plane showing rotation B from figure 1.5. The results the following ranges for the delivery systems in the Y-axis: for the Medtronics DS a range of $3.2° < Y_{angle} < 15.5°$, for the Edwards DS a range of $3.6° < Y_{angle} < 11.8°$ and a range of $7.8° < Y_{angle} < 34.9°$ for the prototype.

The rotation around the X-axis is visible during the experimental run for the Edwards DS and the prototype in figure 3.4. This rotation represents rotation the frontal plane showing rotation A from figure 1.5. In the plot it is also visible that the prototype has a bigger reach with a range of $6.4° < X_{angle} < 38.4°$ for the prototype compared to a reach of $3.7° < X_{angle} < 32.5°$ of the Edwards DS.

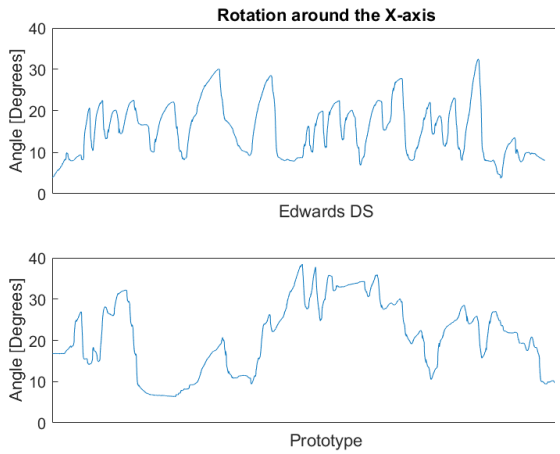

Figure 3.4: The rotation around the X-axis for the Edwards DS and the prototype during the experimental run.

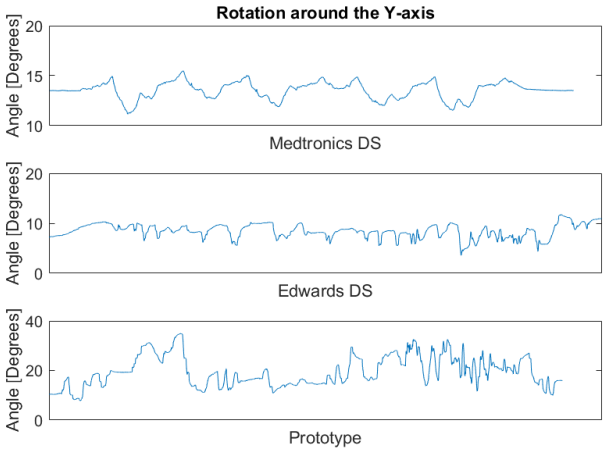

Figure 3.5: The rotation around the Y-axis for each delivery system during the experimental run.

3.4.2. Technical test 2

The final positions of all the runs for the Medtronic DS, Edwards DS and the prototype are plotted in the ZY-plane in figure 3.7, 3.9 and 3.11 respectively. It is visible that the Medtronics DS always has an error in the positive Y-direction. Moreover, the Edwards DS and the prototype which are steerable in this plane, have a smaller error in the Y-direction. Another interesting observation is that all the delivery systems overshoot the target point (illustrated in blue) in the Z-direction.

The table showing the errors for the tip of the delivery system compared to the reference point of each run is visible in figure 5.10 in Appendix 5.4 and shows that the prototype has the smallest error compared to the Medtronics and Edwards DS. Interesting to see is that the error for the Medtronics and the Edwards system is almost the same.

Lastly, all the experimental runs are plotted in figure 3.6 and shows the angle in which the tip was aligned in the final position compared to the reference point in the XZ-plane. The plot shows that the Edwards and the Medtronic system cannot achieve the rotation in the XZ-plane to provide a coaxial alignment in the XZ-plane. In addition, the results show that the prototype does achieve a coaxial alignment in the XZ-plane but not for every run.

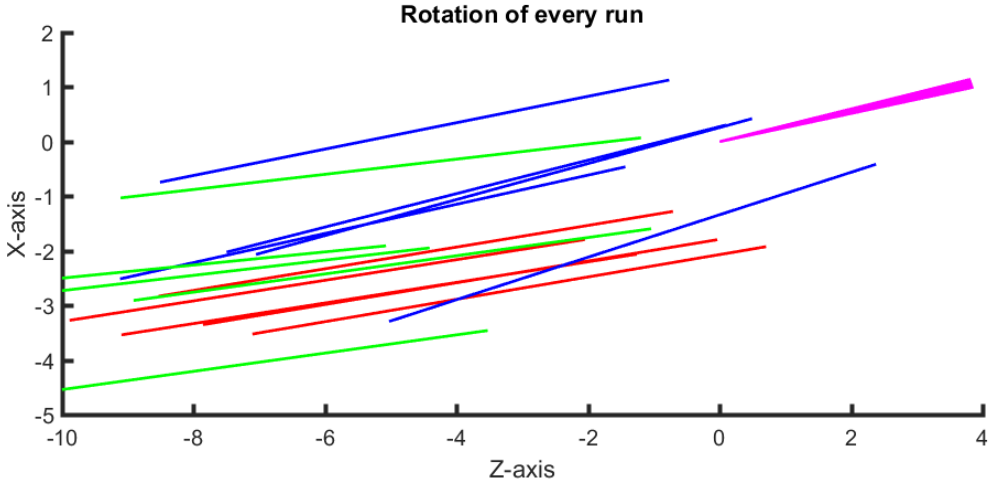

Figure 3.6: The final oriëntation of each run in the XZ-plane for the Medtronics DS (Red), the Edwards DS(Green) and the Prototype (Blue) compared to the Reference point (Magenta).

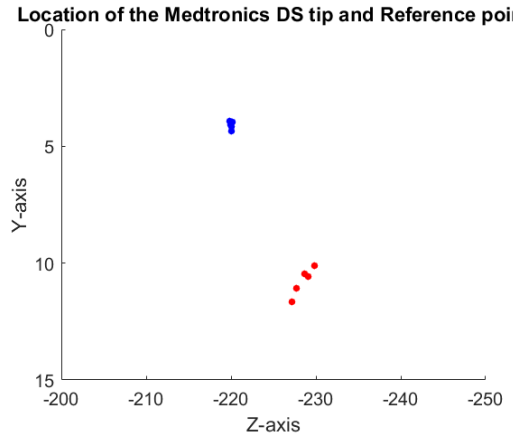

Figure 3.7: Showing the final position of the tip of the Medtronic DS in the YZ-plane in red relatively to the reference point in blue.

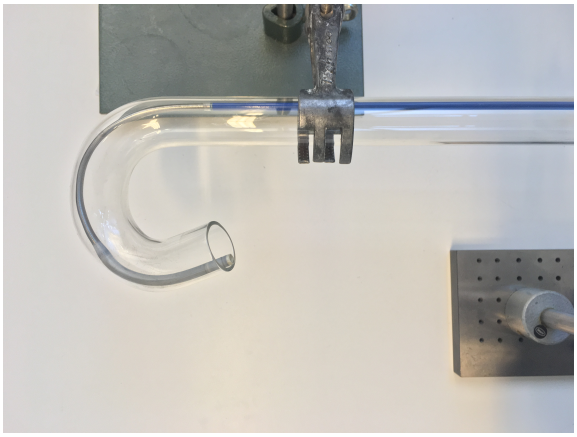

Figure 3.8: Showing 1 run of the Medtronics DS in the frontal plane of the aorta model.

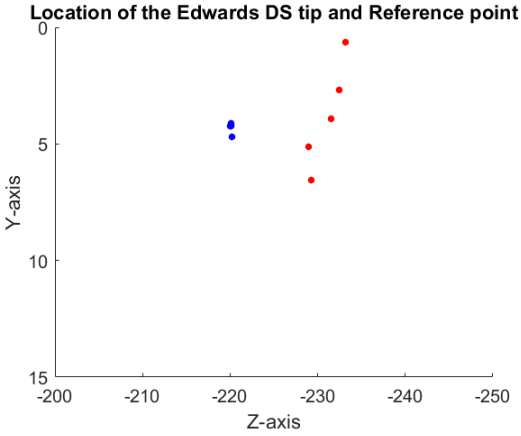

Figure 3.9: Showing the final position of the tip of the Edwards DS in the YZ-plane in red relatively to the reference point in blue.

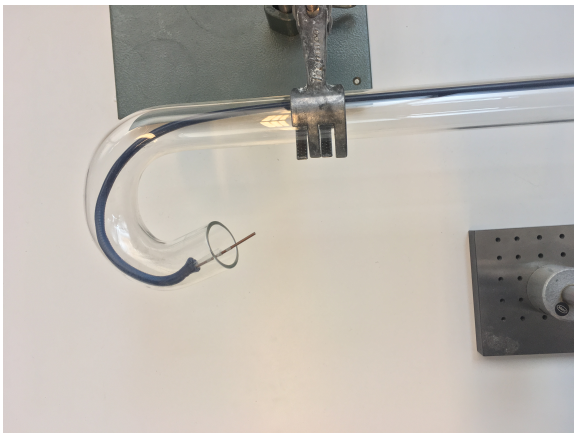

Figure 3.10: Showing 1 run of the Edwards DS in the frontal plane of the aorta model.

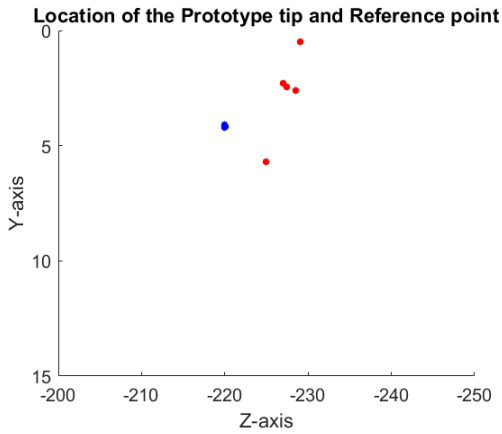

Figure 3.11: Showing the final position of the tip of the prototype in the YZ-plane in red relatively to the reference point in blue.

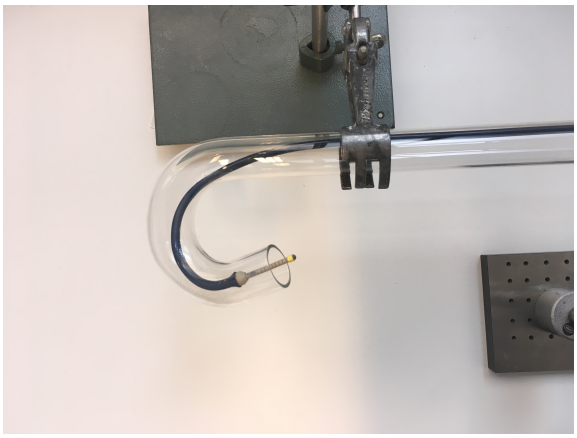

Figure 3.12: Showing 1 run of the prototype in the frontal plane of the aorta model.

3.4.3. User Test

During this experiment it became clear that the surgeons prefer an oblique implantation and the reason is depicted in figure 3.14. By implanting the Edwards Sapiën valve in this oriëntation, the surgeons find support for the outer catheter on the aorta wall, indicated by the red arrow. This point of support ensures that the DS doesn't move upwards back into the aortic arch when the heart valve is pushed down into the aortic annulus by the inner catheter during the operation. When asked to manoeuvre the prototype to the reference point, the surgeons still handled the prototype as the Edwards DS, despite the explanation of the modification that's incorporated in the prototype. When asked why they still prefer the oblique implantation of the tip of the prototype, the explanation above was given.

	Medtronics DS		**Edwards DS**		**Prototype**	
	X-axis	Y-axis	X-axis	Y-axis	X-axis	Y-axis
Run 1	3,92	5,06	1,18	7,87	3,37	2,05
Run 2	4,84	3,97	10,77	8,32	0,40	5,34
Run 3	4,31	3,10	6,07	7,61	3,78	2,00
Run 4	3,54	4,88	4,44	7,23	5,21	1,75
Run 5	4,51	4,98	3,76	6,84	5,36	0,68
Mean	4,22	4,40	5,24	7,57	3,63	2,36

Figure 3.13: Table of the rotational errors in degrees for the 3 delivery systems

After the question what happens if the heart valve is not properly anchored or there is aortic ragurgitation they explained the following. They look at the ultrasound recordings during surgery if there is regurgitation after deployment of the heart valve prosthesis. If there is regurgitation, they try to decrease the amount of regurgitation by repeated balloon valvuloplasty to push the stent of the valve firmer into the aortic annulus.

Moreover, they confirm that the Medtronics DS doesn't have the possibility to be steered in any way and they explain that the implantation depth is important for the success of the implantation of the Corevalve. The preference of the surgeons goes to the Edwards DS because the steer ability makes it easier to manoeuvre the heart valve in the correct position. They add that it has to be kept in mind that the route to the aortic annulus can be tortuous and the native aortic valve can make it difficult to move the tip of the delivery system through the aortic annulus. These are the reasons that they prefer the extra steer ability of the Edwards DS, because it gives them more possibilities to manipulate the tip.

They experienced the experiment as interesting, because this is the fist time they can actually see real time how the tip of the different delivery systems react to manipulations of the handle of each delivery system. They explain that they normally don't really see how the tip reacts to manipulations of the handle because they only look at the imaging techniques, which are limited. This confirms the findings in the literature that the imaging techniques are still a limiting factor on the positioning of the heart valve prosthesis in the TAVI procedure [9].

3.5. Discussion/Conclusion

The first research goal is accomplished by the development of a prototype with an extra steerable rotation in the tip compared to the Edwards catheter. The second research goal has to be completed which is the validation of the functionality of the prototype. This experiment will validate the functionality of the prototype by comparing to the current delivery systems with the prototype with regards to the positioning of the distal tip.

To validate this functionality, the tips of the prototype and the current Edwards and Medtronics delivery systems were tracked when they were manoeuvred through a glass aorta model to the aortic annulus of the model. Two tests were performed to validate the functionality. First, the reach of the three systems in the aortic annulus were compared to give an image on the possibilities the three systems give. Second, the three systems were compared in an experiment where the task was to position the tip of the delivery system in the same configuration as the reference point. In this case

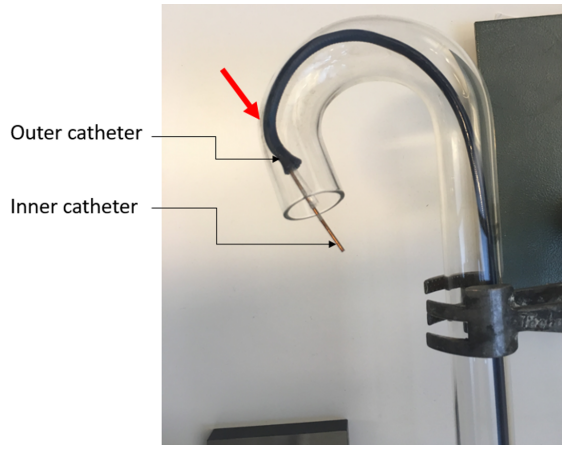

Figure 3.14: Showing the preferable implantation coördination of the tip of the Edwards DS of the surgeons.

Figure 3.15: Showing the structure of the tip of the Edwards DS where the heart valve prosthesis is placed in.

the reference point represented the perfect position for the heart valve prosthesis to be deployed in the aortic annulus.

Figures 3.3 clearly shows the difference in reach between the three systems. It is important to realize that the view is from inside the aorta lumen looking from the ascending aorta to the aortic annulus. The Medtronics DS, which is not steerable, will always remain on the outside of the lumen of the aorta because it doesn't have the possibility to be steered in any way. This finding is also supported by figure 3.8. The plot of the Edwards DS shows that the tip can be steered to the inside of the lumen of the aorta in the YZ-plane. If a close look is taken, it is visible that two pathways are formed. This is realized by rotating the outer catheter. This rotation will produces torque in the catheter and moves the tip slightly up and downwards. Lastly, the reach of the tip of the prototype is visible in the third plot and this shows a greater reach compared to the current delivery systems. This has multiple reasons. First, the tip of the prototype is steerable with two rotations, which gives more possibilities to steer the tip of the DS. Second, the absence of the inner catheter in the prototype resulted in more flexibility in the distal part of the DS and consequently had a positive effect on the reach of the tip of the prototype. This is supported if a closer look is taken to the plots of the Edwards DS and the prototype in figure 3.3 where it is visible that the Edwards DS cannot reach to both sides of the lumen completely and the prototype can.

The second parameter that was measured was the angle of the tip of the delivery system. The rotation around the X-axis is the rotation in the frontal plane, also referred to as rotation A in this report. The results are plotted in figure 3.4 and show that the prototype can be positioned in a bigger range of angles than the Edwards catheter. This is due to the fact that the inner catheter is removed in the prototype, which resulted in more flexibility in the tip of the prototype than the Edwards DS.

In figure 3.5 the rotation around the Y-axis was measured for the three systems. This rotation represents the rotation in the sagittal plane (rotation B). If the achieved angles of rotation around the Y-axis for the Edwards DS and the prototype are compared it is clear that the prototype covers a bigger range in possible angle oriëntations (Edwards: $3.6^\circ < Y_{angle} < 11.8^\circ$) ; prototype:($7.8^\circ < Y_{angle} < 34.9^\circ$). This is expected because the prototype has an extra steerable rotation to control rotation in this plane. Another interesting finding in these results is the rotation of the Edwards system compared to the aorta model. The angle oriëntation of the aorta model relatively to the Aurora system was measured at the start of the experiment and gave a rotation of 17.7° around the Y-axis. The plot of the Edwards DS in figure 3.5 shows that the DS couldn't manage the required rotation of $17.7\circ$ to get a coaxial placement of the tip in the XZ plane. This difference is also depicted in figures 3.16 and 3.17. Moreover, the oriëntation of the tip of the Medtronics system approaches the value of the aorta model, because this system will align with the ascending aorta, visible in figure 3.8.

The results of the first test show that the prototype gives a bigger reach in both the position in the lumen of the aorta, as the angles in which the tip can be configured. However, this doesn't give a direct answer to the research question stated in chapter 1.2 if the prototype ensures a better positioning. It is not visible if these possibilities in angle and position provide the ability to steer the tip to the

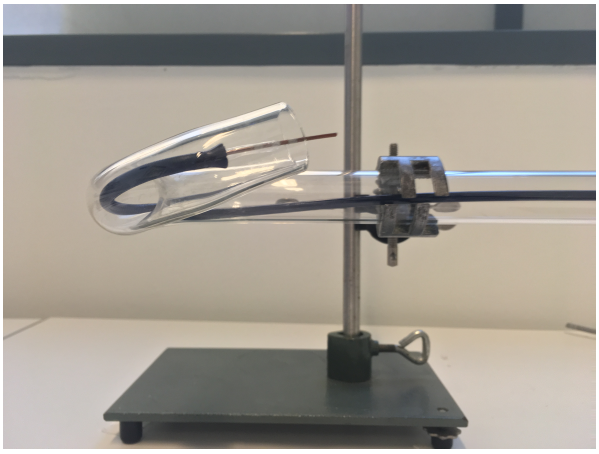

Figure 3.16: Showing the oriëntation of the Edwards DS in the aorta model in the sagittal plane.

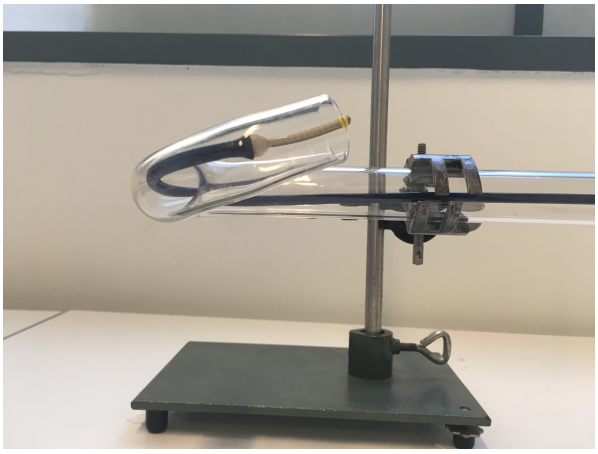

Figure 3.17: Showing the oriëntation of the prototype in the aorta model in the sagittal plane.

configuration needed for a perfect implantation. Where the perfect oriëntation is in the center of the aortic annulus in a coaxial oriëntation.

Technical test 2 is performed to answer this question. The task in this test is to manoeuvre each DS to the reference point. The reference point represents the center of the aorta lumen, coaxial to the aortic annulus. The results of the position of the tip of each delivery system for each run is plotted in figures 3.9, 3.7 and 3.11 in the YZ-plane. Figure 3.7 shows that the Medtronics DS can only remain at the outside of the lumen of the aorta. Figures 3.9 and 3.11 show that the tip can be steered to the center of the lumen towards the reference point depicted in blue.

It is visible that the tip always overshoots the target in the Z-direction in table 5.10. For every delivery system the error on the z-axis is the largest. This can be attributed to the fact that the implantation depth is not clearly visible for the user based on the shape of the phantom model. This also represents the reality where, as explained in appendix 5.3, the imaging techniques are insufficient to determine the exact location of the aortic annulus.

The mean square error of 8.1 mm for the prototype is smaller than the Medtronics and Edwards system with 11.3 mm and 11.6 mm respectively. This implies that the tip of the prototype can be steered better to the desired position. The error for the Medtronics and the Edwards system is almost the same which is not expected because the Edwards DS has an extra steerability compared to the Medtronics DS which should result in a smaller error.

The explanation for this finding is visible in table 5.10. This table shows the errors on all three axis for the three delivery systems. It shows that the error for the Edwards catheter is caused by the large error on the Z-axis compared to the Medtronics DS and the prototype. If only the mean error on the on the x- and y-axis are compared within the three systems, it shows that the Medtronics has the largest error on the x-axis as (3.3 mm) well as the y-axis (6.7 mm) compared to the prototype (x = 2.1 mm, y = 2.0 mm) and the Edwards DS (x = 2.9 mm, y = 1.6 mm).

Table 3.13 shows the error of the oriëntation of the tip in the final position compared to the reference point. It shows the smallest rotational errors for the prototype compared to the Edwards and Medtronics DS. The biggest rotational errors are achieved by the Edwards DS. This can be attributed to the fact that the main focus of the user is to position the tip in the center of the aorta lumen rather than coaxial to the aortic annulus. To achieve this target the handle of the Edwards DS had to be rotated to produce torque in the outer catheter which moves the tip of the Edwards DS in positive x-direction. Moreover, the Edwards DS is stiffer than the prototype which forces the user to find support at the wall of the aorta, as is depicted in figure 3.14, and produce torque in the outer catheter which resulted in a movement of the tip towards the center of the lumen when the delivery system was pushed upwards into the aorta. As a result the rotation around the x-axis increases, which is visible in figure 3.14.

The error in the x-axis is largest for the Edwards DS. This is also attributed to the produced torque in the outer catheter to move the tip more to the center, but the inability to adjust the angle in the sagittal plane, visualized in figures 3.16 and 3.17. The extra rotation of the prototype clearly demonstrates the improvement of the modification on the prototype. The results presented in table 3.13 also support

this finding with the smallest rotational error for the prototype.

The research question of this report is if an extra rotation provides a better ability to position the tip coaxial in the center of the aortic annulus. This research question can be confirmed because the rotational error together with the location error is the smallest for the prototype if it is compared to the Medtronics and Edwards delivery systems.

4

Discussion

The trend in the treatment of aortic stenosis is moving towards the TAVI procedure [4]. During this procedure a stent with a heart valve prosthesis is wedged over the aortic valve that is calcified. The access route towards the aortic valve is through the groin and iliac arteries via the aorta to the aortic annulus. Delivery systems mounted with the crimped heart valve prosthesis are pushed up through this access route to deploy the prosthesis over the aortic annulus.

The first goal of this research is to deliver a prototype that can be steered with two rotations appointed in figure 4.2. The Edwards DS, that is already used for the TAVI procedure, was disassembled to explore the current proven techniques that were used for the TAVI procedure (see chapter 2.1). The described mechanism for the rotation in the Edwards DS is a proven concept and therefore chosen as the mechanism to provide the second rotation. This second rotation had to be incorporated into an isolated part of the Edwards delivery system depicted in figure 2.4. After two experiments, a PEEK catheter strip is selected and added to the prototype together with a modification in the handle. This resulted in the prototype that is described in chapter 2.4 that will be validated and used for the answering of the research question.

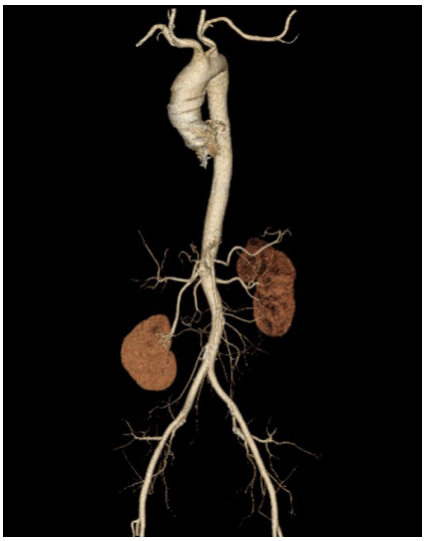

Figure 4.1: The anatomy of the aorta in the human body showing the route from the iliac artery, which is the starting point for the TAVI procedure, to the aortic annulus.

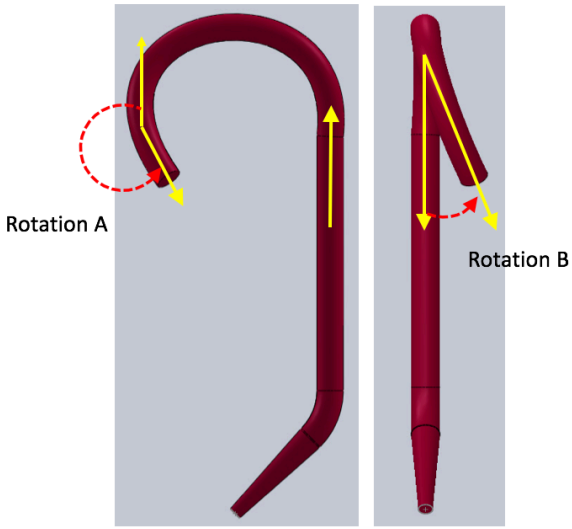

Figure 4.2: A simplified model of the route from the iliac artery to the aortic annulus with on the left hand side a frontal view and on the right hand side a sagittal view. The two rotations that are referred to in this research are depicted as rotation A and rotation B.

The rotations and the location of the tip in the aorta model are important during this discussion. Figure 4.2 shows the rotations that are appointed too during this discussion. Rotation A represents

the rotation in the frontal plane and rotation B is the rotation in the sagittal plane of the model. The location error as well as the rotational error will be discussed between the three delivery systems.

The results of the first test in the validation experiment show that the prototype was more flexible to perform rotation A. This is accounted to the removal of the inner catheter of the Edwards DS. This improved flexibility is beneficial when the patient has a more horizontal oriëntated aorta. Chan et al. explained that the TAVI procedure is difficult in patients with a more horizontal oriëntated aorta [6]. If we look at the validation study, this could be explained by the stiffness in the distal part of the Edwards DS, resulting in an insufficient rotation to align the heart valve prosthesis in the frontal plane to the aortic annulus.

The extra flexibility of the prototype to perform rotation A together with the extra steerable rotation B, clearly showed an improved reach of the prototype compared to the current delivery systems. The improved possibilities in which the tip could be oriëntated is visible in figures 3.3, 3.4 and 3.5. This improved reach in the aorta lumen does not directly prove that the tip of the catheter has the ability to be steered to the center of the aorta lumen, coaxial to the aortic annulus. For this to happen, the combination of the location at the center of the lumen and the coaxial oriëntation has to be realized. Therefore, the second technical test is performed to validate the ability to steer the tip of the DS in the perfect position.

The results show the largest error in the rotation around the y-axis for the Edwards DS. This is accounted to the incapability to rotate the tip in the sagittal plane of the model. The prototype does provide this rotation and the difference is illustrated in figures 3.17 and 3.16.

Moreover, the rotational error of the Edwards DS in the frontal plane is biggest error compared within the 3 delivery systems. This is accounted to the stiffness of the distal part of the DS. This stiffness causes the need to find support at the wall of the model, depicted in figure 3.14, to steer the tip to the center of the aorta lumen. This need for support causes the misalignment of the Edwards DS tip in the frontal plane visualized in figure 3.14. The prototype didn't need this support, which is also clearly visible in figures 3.12. This picture shows an alignment in the frontal plane without contact between the delivery system and the wall in the aortic arch.

The validation study shows the smallest error for the rotation as well as the location of the prototype. This is a clear indicator that the extra steerability and design improvements of the prototype regarding the flexibility has a positive effect on the ability to position the tip of the delivery system, which in the end will determine the position of the heart valve prosthesis.

Optimal placement of the prosthesis prolongs the lifespan of the prosthesis, because the stresses on the leaflets of the prosthesis are minimized [32]. Currently, the TAVI procedure is only performed on intermediate and high-risk patient which are mostly elderly, but when the TAVI procedure is going to be performed on younger and lower risk patients the lifespan of the prosthesis for the TAVI procedure has to be maximized. In addition, this improved positioning will ensure a better anchoring of the heart valve prosthesis in the aortic annulus, which minimizes chances on dislocation, conduction disturbances and regurgitation [9, 22].

The surgeons also performed the experiment in a user test. An interesting finding during the experiment was that the surgeons implant the valve in an oblique oriëntation to find support at the aorta wall to push the prosthesis forward to control the implantation depth, explained in chapter 3.4.3. It is explained that they find solutions to the incapabilities of the tools that are provided, which are in this case the Medtronics Corevalve and the Edwards Sapiën.

They also explain that the skewed implantation in the sagittal plane is currently not always visible for the surgeons because the imaging techniques are in 2D. This is demonstrated by example B and C in figure 4.3. If the surgeons have a 2D image they define the implantation depth as the distance demonstrated by the arrows in example C. But if the view is rotated, illustrated by example B, it is visible that the prosthesis is skewed in the aortic annulus and could have an insufficient anchoring as a result. This example shows that a coaxial placement to the aortic annulus is needed for the most optimal anchoring of the heart valve.

The limitation of the validation study is that the aorta model in which the experiment was conducted was made out of glass. Glass is solid and differs greatly from the aorta in the human body. This could lead to other behaviour of the delivery systems because glass will give more resistance when the delivery system is pushed against the glass wall compared to the human aorta wall. Moreover, the glass is smooth and straight where in the human body tortuosity is very common together with possible obstructions like calcifications or cholesterol. In addition, a limitation of the aorta model is that

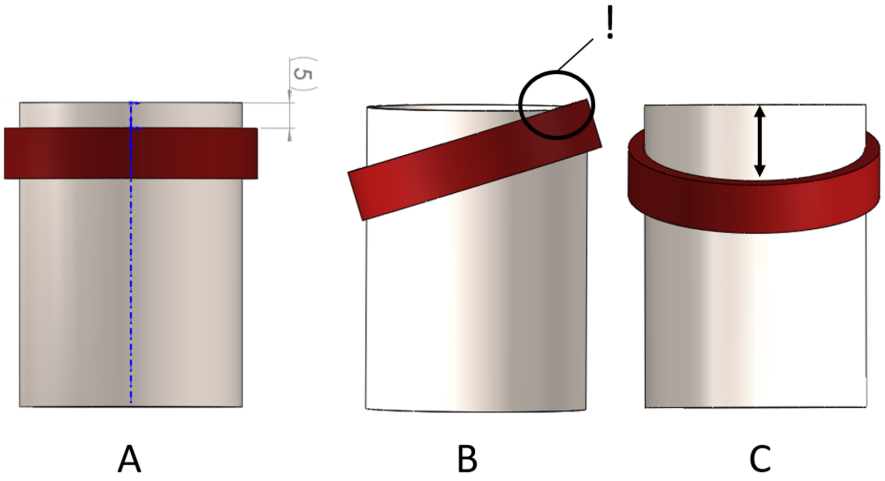

Figure 4.3: Example of the consequences of a skewed implantation. The red ring represents the aortic annulus and the cylinder is the stent of the heart valve prosthesis. The left ventricle is at the top of the picture and the aortic annulus is bottom of the picture. Example A shows the desired implantation 5 mm below the aortic annulus. Examples B and C is the same implantation but example B is a view in the sagittal plane and example C is a frontal view.

it represents the average dimensions of the human aorta geometry whereas the delivery systems have to function in all the patiënts with different geometries of the aorta. A follow up study is needed in different models with varying geometries of the aorta to determine the functionality of the prototype.

Moreover, the glass model is not a representation of the human aorta concerning the environment. During the operation the delivery system is inserted and positioned in the presence of blood flow. Despite the fact that rapid pacing of the heart is performed during the deployment of the heart valve, causing the blood flow to be minimized, the prototype does need validation under these circumstances to see the effects of a dynamic and wet environment [9].

There are a few limitations on the design of the prototype which have to be addressed in future development. The part of the handle that controls rotation B has to be rotated multiple times to create movement of the tip. This is due to the fact that rotation A is created by shortening of the tension wire. The shortening of this wire consequently shortens the wire that causes rotation B. The handle mechanism for rotation B currently has to compensate for this shortening by rotating the wheel multiple times. A mechanism has to be created in which the shortening of the pulling wire for rotation A also leads to the shorting of the pulling wire for rotation B, but rotation B still has to be controlled separately.

Another problem that has to be addressed is that the length of the modification at the tip of the prototype. This modification was designed to fit to the isolated Edwards system, but in future development both rotations have to be incorporated into one material. Taking into account the addition of an inner catheter for the control of the implantation depth and the possibility to inflate the balloon for balloon valvuloplasty.

Conclusion

In conclusion, the research question can be confirmed because the prototype with the extra rotation in the distal part of the delivery system improves the ability to steer the tip to the center of the aortic annulus in a coaxial oriëntation. The study showed that the rotational error as well as the location error was the smallest for the prototype if it is compared to the current techniques. This improved ability to position the heart valve prosthesis in the aortic annulus could improve the anchoring of the heart valve prosthesis. This improvement could reduce aortic regurgitation, rate of wear of the prosthesis and chances on dislocation and conduction disturbances.

5

Appendix

5.1. TAVI procedure

5.1.1. Screening of the patient

Transcatheter aortic valve implantation is a minimal invasive alternative for the treatment of aortic stenosis. The technique is relatively new, so only high-risk patient are selected for this treatment until the long term results show that this procedure is trustworthy [32]. Patient screening is very important when it comes to this procedure but, as figure 5.1 also illustrates, also very difficult [30]. As said before, the procedure is only done for high-risk patients with severe symptomatic aortic stenosis [20]. An interdisciplinary team of cardiovascular surgeons, invasive cardiologists, anaesthesiologists and cardiac imaging specialists perform a screening to determine if the patient is anatomical suitable for this procedure. This screening include coronary angiography; aortography and peripheral angiography of bot iliac and femoral vessels; transthoracic echocardiography; noncontrast-enhanced multislice computer tomography scan of the chest and abdomen to assess aortic, iliac and femoral calcification; lung function tests; carotid artery duplex scan; followed by independent assessment by both a cardiac surgeon and an interventional cardiologist [3].

The presence and severity of ilio-femoral disease is determined together with the feasibility of the TAVI procedure. Catheters and sheaths will be inserted through the arteries, so it's important to determine the minimal lumen diameter, tortuosity and calcification of the arteries that form the access routes to the aortic valve to determine the risk for vascular injury [22]. The transfemoral approach is preferable because of its less invasive nature, but the femoral vascular access has to exceed a diameter of 6 mm because the introduction sheaths used for the TAVI procedure have a minimal diameter of 6 mm. If the diameter is smaller than 6 mm, or if heavy calcification or tortuosity is present, two alternative access routes for minimally invasive techniques are available including the transapical and the subclavian access route. These access routes can be considered when the risks of complications via the transfemoral approach are too high [5].

5.1.2. TAVI procedure transfemoral access route

The transfemoral access route is the default strategy because it's the least invasive approach within TAVI. This approach is associated with greater patient comfort and potentially lower costs as a result of the shorter hospital stay [8]. In the beginning a surgical cut-down was needed to expose the iliac artery. This procedure shifted to a purely percutaneous access via the femoral artery resulting in the least minimal invasive access route available. This retrograde implantation through the femoral access route was first described by Webb et al. for the balloon-expandable valve and nowadays it's used in up to 80% of the cases [8**?**].

The body is thoroughly scanned for potential obstructions in the access route and, based on this screening, the right equipment is selected. When the patient is prepared for the surgery and anesthetized, the femoral artery is punctured with a 0.0035 inch wire followed by an incision of the skin and dissection of the subcutaneous tissue. The femoral artery is predilated and a preclosure suture device is inserted together with a 9-10 Fr sheath over the guidewire to minimize backside bleeding. The wire is exchanged for a soft guidewire and pushed upwards through the aorta into the left ventricle. When

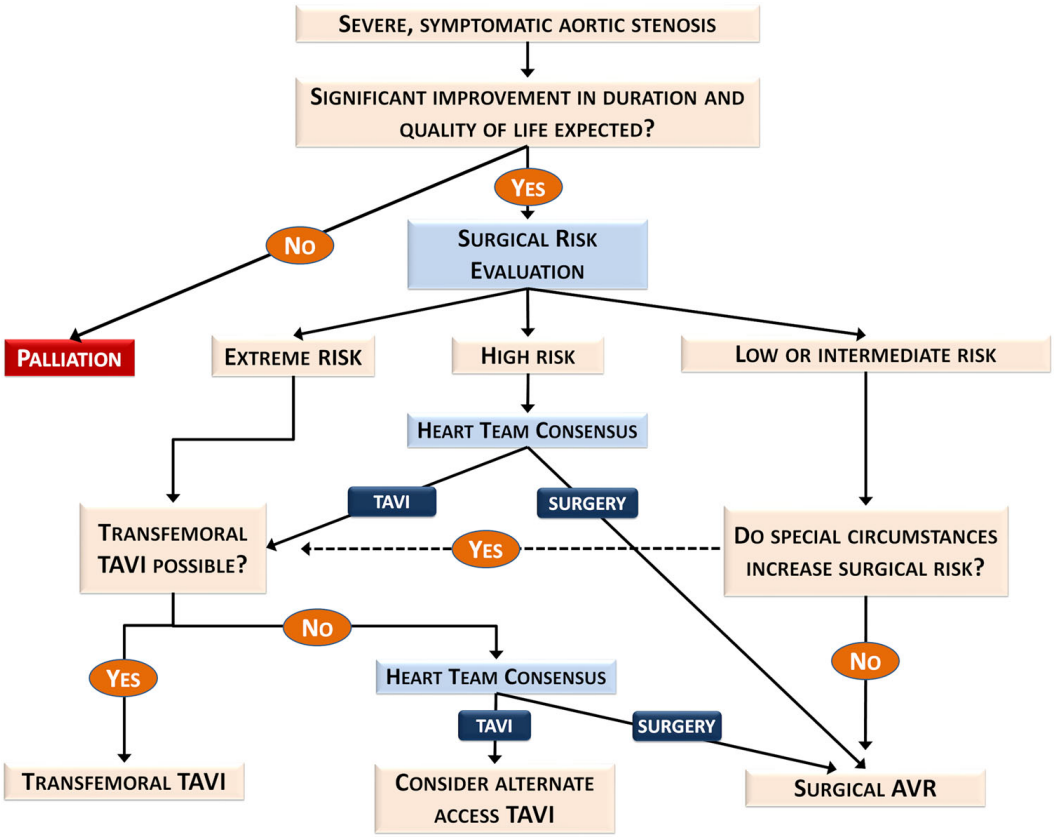

Figure 5.1: Clinical decision algorithm for patients with severe symptomatic aortic stenosis [37]

the tip of the soft guidewire is in the left ventricle, a catheter is pushed over the soft guidewire and lastly the soft guidewire is exchanged for a stiff guidewire. The catheter is removed and a delivery sheath is pushed up until the descending aorta. During all these steps there is contrast fluid added when needed by means of a pigtail catheter that is entered through the other groin. This guidance helps to decrease the chance of puncturing the arterial wall with the catheters and guidewires and accurately place the valve over the native aortic valve [32].

The set-up is now ready to insert the aortic valve that's crimped onto the delivery catheter. This delivery catheter is pushed through the delivery sheat and over the stiff guidewire. The valve is released or manipulated, dependent on the type of valve, from its crimped orientation to the extended orientation. The deployment of the valves is performed during rapid ventricular pacing between 160 and 220 bpm to ensures a decrease of systolic blood pressure. Afterwards, the delivery catheter is withdrawn together with the guidewire and delivery sheath that was still in the descending aorta and the puncture sites are closed.

After the access route has been decided, the appropriate valve can be selected. Currently two valve systems are approved for TAVI and are commercially available in Europe, the Edwards Sapiën XT™ (Edwards Lifesciences, Irvine, CA, USA) and the Medtronic CoreValve™ Revalving system (Medtronic Inc, Minneapolis, MN, USA) [3]. The Edwards is a trileaflet bovine xenovalve, which is mounted in a balloon-expandable cobalt chromium stent frame, the Medtronic is a self-expandable prosthesis consisting of a porcine trileaflet valve mounted within a Nitinol stent frame [34].

5.2. Aortic dimensions of glass model

In section 3 the performance of the delivery systems is going to be validated. To research the performance of the delivery systems, an aortic model is made out of glass, to mimic the access route to the aortic annulus. Glass is chosen for time and financial reasons and because it can be easily manipulated into the desired dimensions for the aortic phantom model. A small literature research is done to define the dimensions of the aortic model. The dimensions of the aortic arch are most important because in this part of the access route, the steerability is needed to manoeuvre the heart valve to the aortic annulus. The current Edwards and Medtronic delivery systems, that are used for the validation study, are also designed to function in the human anatomy, so a realistic model has to be created.

	Age <30 Yrs	Age >70 Yrs
Ascending aorta diameter, mm	27.5 ± 2.8	33.2 ± 4.3
Aortic arch length, mm	100.4 ± 7.1	130.9 ± 13.9
Aortic arch width, mm	58.6 ± 4.7	78.5 ± 8.7
Aortic arch height, mm	34.3 ± 2.9	41.5 ± 4.5
Aortic arch curvature, mm^{-1}	0.034 ± 0.002	0.027 ± 0.003
Proximal descending aorta diameter, mm	20.5 ± 1.6	24.3 ± 2.7
Distal descending aorta diameter, mm	18.3 ± 1.4	21.5 ± 3.2
Descending aorta length, mm	139.3 ± 15.8	142.6 ± 13.3

Figure 5.2: Table with the values for the geometry of the aorta [28].

Figure 5.3 shows how the dimensions of the aortic arch are defined in a lot of articles. Redheuil et al. did research into the dimensions of the aortic arch geometry and the age related changes in this geometry [28]. They studied 100 subjects (55 women, 45 men, average age 46 ± 16 years) using MRI to determine the arch geometry. Their findings are displayed in table 5.5.

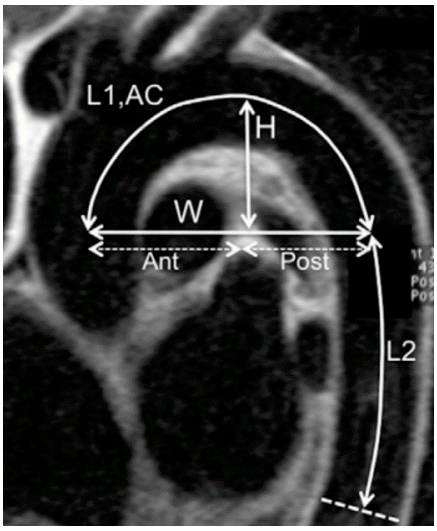

Figure 5.3: AC= average arch curvature; Ant= anterior arch width; H= arch height; L1= length of the aortic arch; L2= length of the descending aorta; Post= posterior arch width; and W= arch width.

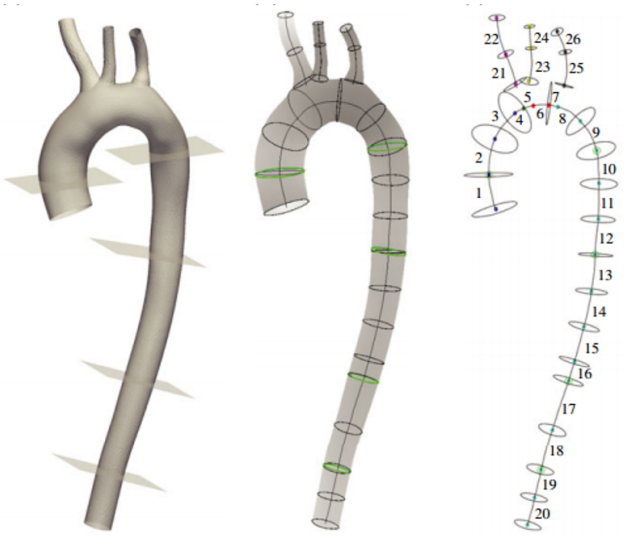

Figure 5.4: 3D geometry and planes corresponding to the MRI flow/area measurements. Centerlines and contours (black) used for the definition of the 1D geometry and the contours (green) corresponding to the MRI measurements [1].

Alastruey et al. also researched the haemodynamics together with the geometry of the aortic arch [1]. They used MRI to determine the geometry and divided the aorta into different sections and defined each section of the aorta in length, diameter and the flow rate. The division of the sections is visible

in figure 5.4. They corrected the 3D arterial geometry based on five 2D area measurements and came up with the figure on the right to define the contours of the geometry. Five planes are highlighted in green and the 1st green cross section is situated in the ascending aorta and the fifth in the end of the descending aorta. They found a bad fit between the first and second green section. They described this bad fit could be explained when the plane perpendicular to the frontal plane was checked. Here, a 17 degree difference in plane configuration was visible, implying an angle of 17 degrees in the sagittal plane between the ascending and descendi ng aorta.

Combining the information from Alastruey et al., Redheuil et al and Mestres et al. [1, 23, 28]. the model in figure 5.5 is defined as a realistic reflection of the anatomic aorta geometry. This model will be made out of glass to mimic the access route to the aortic annulus.

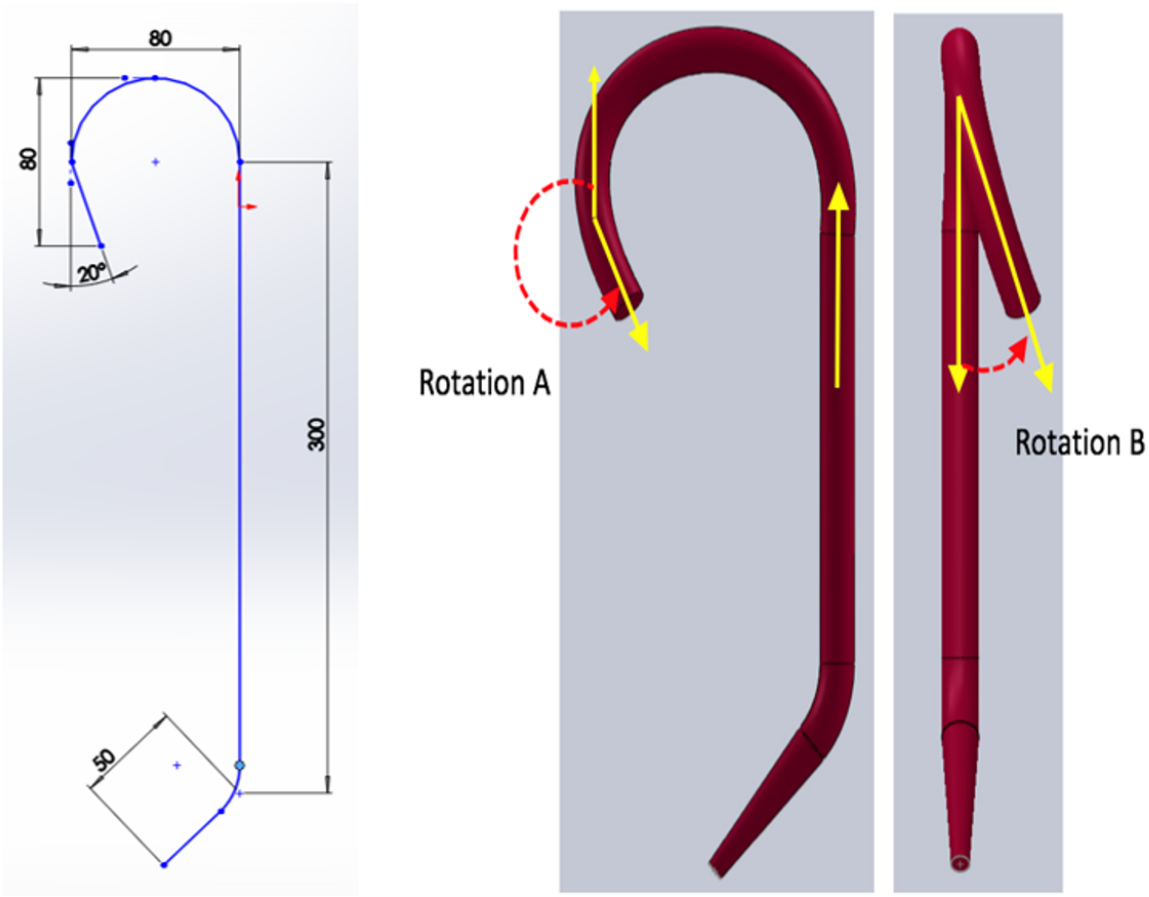

Figure 5.5: The dimension chosen for the glass model of the aorta given in a rendering of a SolidWorks drawing. The dimensions given in the figure are the dimensions of the centerline of the aorta model.

5.3. Importance of positioning

When the aortic arch is passed with the delivery catheter, the prosthesis has to be accurately positioned over the native aortic valve to achieve optimal results and to minimize complications [9, 22, 29]. This positioning is complicated by the nature of the procedure, because a thin delivery catheter has to moved over a long distance, with a few bends, and still be maneuverable at the distal part of the delivery system. The optimal function of the prosthesis relies on correct sizing, correct positioning of the prosthesis and lastly the appropriate expansion and apposition of the prosthesis to the surrounding tissue [31]. Determining the optimal deployment of the prosthesis can be assessed by measuring the two most important parameters after implantation: the residual gradient and the degree of aortic regurgitation. These parameters are dependent on the configuration of the prosthesis that can be divided into: the implantation depth and angle relative to the aortic annulus, as well as the displacement of the native leaflets relative to the coronary tree. If there's still a residual gradient or significant regurgitation, they way in which the prosthesis is misplaced has to be identified. An oblique implanted prosthesis or a too low or high implantation can have different consequences like for example: transaortic regurgitation, dislocation of the prosthesis, embolization and conduction disorders [9]. These effects on the misplacement of the prosthesis together with the clinical problems are discussed in this chapter using the results of different studies.

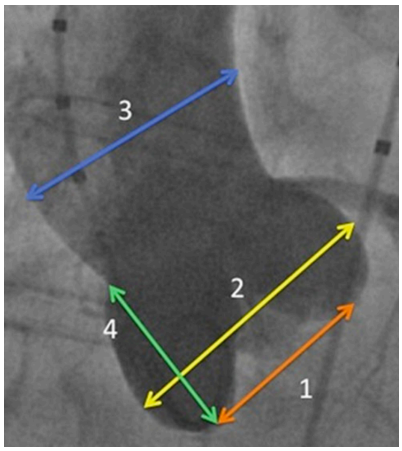

Figure 5.6: Points of interest of the aortic annulus.

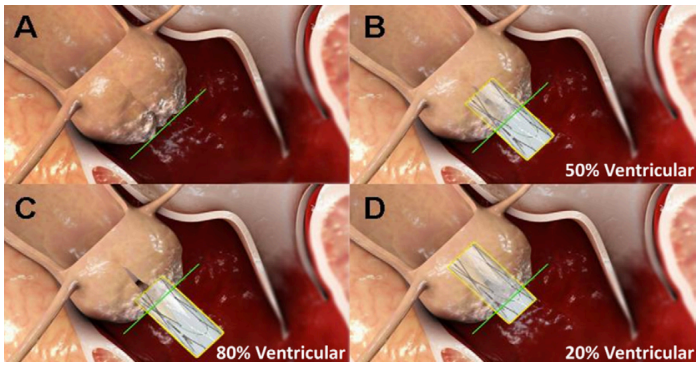

Figure 5.7: Device positioning in percentages relatively to the aortic annulus

5.3.1. Implantation depth

Firstly, the implant depth is very important for the proper functioning of the valve. The implant depth relative to the aortic annulus is determined during the procedure by inserting contrast fluid with a pigtail catheter that's positioned at the annulus level (visible at the crossing of the yellow and green arrow in Figure 5.6. When the fluid is inserted, there's a cloud of contrast fluid visible and the two most distal points indicate the start of the aortic annulus. This is appointed to in figure 5.6 by arrow number 1. The implant depth is important because it could lead to different problems like conduction disturbances, device drop into the aorta or left ventricle, device embolization, coronary flow obstruction and paravalvular leakage [9].

Groves et al. studied the effects of the implant depth on the valvular hemodynamics [15]. They used a setup that mimics heart function and small particles were used for seeding the flow. Imaging techniques captured the resident time of particles in the left ventricle and the resident time in the sinus of Valsalva. Both are interesting because a high resident time in the left ventricle would insinuate that there is resistance in outflow of blood. Moreover, a low resident time of particles in the sinus of Valsalva could have negative consequences on coronary perfusion [15]. Also the normal and shear stresses in the aorta were examined, as they may result in damage to blood components, potential aortic wall rupture and dissection. Moreover, asymmetry in aortic stresses can cause a post-stenotic dilation [38]. A variation in implant depth from 5mm until 20mm was applied to see the effect of the implant depth on the valvular hemodynamics.

Results showed that normal and shear stresses increased and became more asymmetric when the valve was displaced further than 5 mm. A displacement of 5 mm still gave a symmetrical and a low stress profile, suggesting that the optimal implantation depth is 5 mm. Further displacement resulted in stresses that steadily increased and got a more asymmetrical stress profile. These findings impose deleterious effects on the aorta. In addition, the pericardial leaflets of the valve have a certain lifespan. When more stresses are exerted on these leaflets, the lifespan can be shortened [9].

Implantation depth can also be associated with adverse events such as conduction disturbances [22]. Petronio et al. studied the optimal implantation depth of the Corevalve with a focus on permanent pacemaker implantation [27]. Implantation depth was defined as the maximal distance between the intraventricular end of the prosthesis and the aortic annulus at the level of the noncoronary cusp. A distance smaller than 6 mm was defined as the optimal implantation depth and a distance higher than 6 mm was considered to be a low implantation.

An optimal implantation depth was achieved in 43.2% of a group of 194 patients, with a mean implantation depth of 3.0 $\pm$ 2.2mm. The group with a low implantation depth had a mean of 9.9 $\pm$ 2.2 mm. The total rate of permanent pacemaker implantation was 24.4% and within the group of people with an optimal implantation depth, 13,3% got a permanent pacemaker implantation. This percentage was 21,4% in the group of people with a low implantation. With these results, the study concluded that the only predictor of a permanent pacemaker implantation was a low implantation of the prosthesis [27].

Also Lenders et al. studied the implantation depth of the Corevalve and the effects it had on the conduction disturbances [19]. A lower implantation of 8.9mm $\pm$ 4.2mm resulted in a higher amount of patients that needed a permanent pacemaker implantation compared to a higher implantation of 6.9 $\pm$ 3.8 mm. The cause for these conduction disturbances is stated as trauma to the IV-septum and subsequently to the conduction tissue it embeds. This is induced by the relatively deep implanted frame that is considered to be a major determinant for the conduction disturbances after TAVI. This theory is supported by Petronio et al. in a recent study into the implantation of the Corevalve together with a study of Rodés-Cabau [27, 29]. They explain that the anatomic relationship between the aortic valve and the components of the cardiac conduction system explains the frequent occurrence of conduction defects after interventions of the aortic valve. The Corevalve and the Edwards Sapien valve both have a radial force to anchor the valve into the native aortic valve. This is close to the point where the left bundle branch emerges from the left side of the ventricular septum. Mechanical compression leading to temporary inflammation or permanent damage to the conduction pathways is probably the main determinant of conduction disturbances. Also the need for a permanent pacemaker following the TAVI procedure is variable but with the Corevalve it's a bit higher (>10% in most studies) compared to the Edwards valve (<7%) [29]. The difference can be explained by the stent design from which the Corevalve is 5mm longer than the Edwards valve.

Dvir et al. studied the positioning and small device movements of the Edwards Sapien valve during different stages of deployment in a multi-centre evaluation [9]. The positioning of the Edwards valve is performed during rapid pacing and by balloon expansion. This study measured the movement of the upper part and the lower part over the device regarding the height relatively to the aortic annulus. Figure 5.7 shows how the percentages, concerning the implant depth in the results, are used. Results showed that the position of the valve before balloon inflation was highly correlated with its position after deployment. It showed a significant increase in height from 32.6% ventricular to 16.7%. In 91.2% of the cases the final device location was <40% ventricular. Absolute device movement towards the aorta after deployment and during final rapid pacing was 2 mm $\pm$ 1.43 mm. This upwards movement was asymmetrical, resulting in a shortening of the device. This shortening might have some clinical benefits, because it could decrease the tension on the interventricular septum and possibly reduce the rates of conduction defects [9]. This distance is also found in a study performed by Nietlispatch et al. [24]. This suggests that this shortening of the device has to be taken into account by the surgeons during placement. Otherwise a too high implantation is the result, increasing the chance on coronary obstruction and valve embolization because of an insufficient anchoring of the valve [22].

The study of Dvir et al. also states that the optimal deployment location of the Edwards valve is still controversial. The best results will be gained when full coverage of the aortic leaflets is obtained with secure anchoring at and below the level of insertion of the native valve leaflet [9]. But the precise location of leaflet insertion is not easy to define using current imaging techniques [9]. This is supported by the fact that the anatomic annulus, that is often used as a reference point, is a virtual basal ring

that is formed at the plane of the base of the aortic sinuses, about 1 to 2 mm below the anatomic ventriculoaortic junction [18]. It remains difficult to determine the exact position relative to this virtual ring.

5.3.2. Dislocation

Dislocation of the prosthesis can be a problem after implantation. Geisbusch et al. showed that dislocation didn't occur with the Edwards valve, but 212 patients underwent TAVI with the Corevalve and 10% had a dislocation of the valve. In 16 of these 21 patients, the dislocated Corevalve was retracted into the catheter and positioned again. However, the Corevalve dislocated in 4 patients after it was completely deployed. The Corevalve had to be retracted with a gooseneck catheter into the ascending or descending aorta and a second prosthesis had to be implanted. In two of the patients the Corevalve dislocated after a redilation manoeuvre, which is used to extend the stent more to overcome present aortic regurgitation [13].

A technique that is often used to overcome aortic regurgitation after a too deep implanted prosthesis is described by Ong et al. where a prosthesis that was implanted too deep was pulled back with the snare technique [26]. The prosthesis was pulled upwards into the aorta which resulted in a better pressure gradient in the beginning, but in the end the prosthesis was pulled too far resulting in a dislocation. Great care had to be taken when the prosthesis was pulled backwards, because if the prosthesis was firmly fixed over the native aortic valve, rupture of the aortic valve or dissection of the aorta could occur if the prosthesis was pulled too hard [26].

The table in figure 5.8 gives the number of dislocations of the two different valves in the transfemoral access route out a literature. The table contains a combination of different studies concerning dislocation of the valve and embolization. A total of 3542 patients is described, not counting the patients of Tay et al. where the total amount of patients over 4 years isn't stated, with a total of 76 dislocated valves (2%). This is consistent with the findings of Rodés Cabau et al where was stated that valve dislocation or malposition was found in 6% of the cases in initial first-in-human studies and 2% in recent studies [29]. The most common sites where the valve dislocated into were the ascending aorta (48%), descending aorta (24%), left ventricle (21%), aortic arch (4%) and the transverse aorta (3%). The most common cause of embolization was malpositioning (n=33 [43%]).

The extra actions that have to be taken after a dislocation affect the operation time of the surgery. Geisbusch et al. showed that a dislocated Corevalve resulted in a longer operation time from 77 $\pm$ 31 minutes in the non-dislocation group to 101 $\pm$ 43 minutes in the dislocation group [13]. This longer operation time aids to an increase in fluoroscopy time, amount of contrast agent applied and radiation dose, which can have renal failure as a result [13].

Author	Year publication	Type of Valve	Total amount of patients	Number of dislocations	AO	DA	LV	TA	AA
Ussia et al.	2012	Corevalve	176	7	6	1			
Tay et al.	2011	Edwards Sapien		7		2		2	3
Guerios et al.	2012	Corevalve	412	6	4		2		
Al Ali et al.	2008	Edwards Sapien	170	7	6		1		
Makkar PARTNER 1	2013	Edwards Sapien	2554	28		15	13		
Geisbusch et al.	2010	Corevalve	212	21	21				

Figure 5.8: This table shows the amount of dislocations described in the stated study. It also indicates if the embolization was in the Ascending Aort (AO), Descending Aorta (DA), Left ventricular (LV), Transverse Aorta or the Aortic Arch (AA) [2, 10, 12, 13, 21, 33, 35]

5.3.3. Trauma to the surrounding tissue

Another effect that was found by two studies was trauma to the surrounding tissue because of the force that is exerted on the artery wall when the delivery catheter is pushed upwards to the aortic valve. Nuis et al. found that new conduction abnormalities were associated with increased levels of leukocyte count after TAVI (14.07 vs 10.39 $\times$ 10^9/L,P= 0.001) [25]. They state it is unclear whether these abnormalities concern a causal relationship with damage to tissue during the delivery of the valve to the native aortic valve with the catheters or whether the increase leukocyte count is caused by post-TAVI conditions like frequent pacing. They point out that, if the increased levels are caused by the former, measures should be taken to limit injury and inflammation.

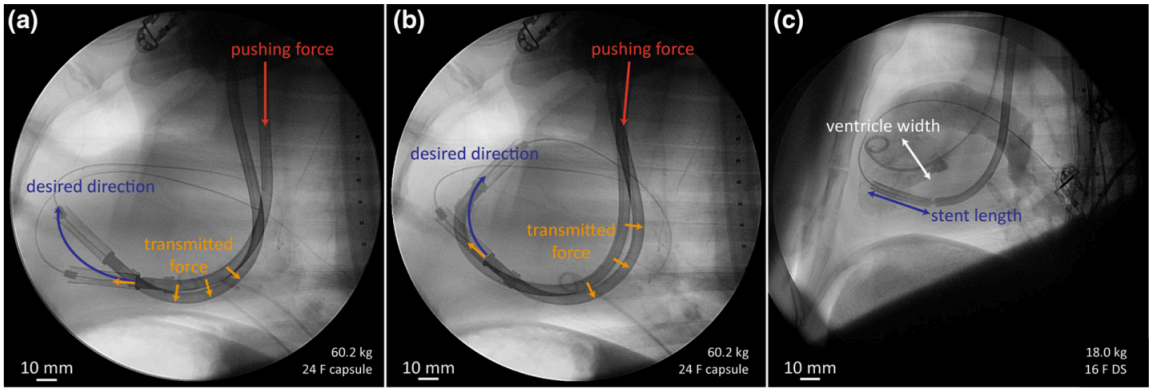

Figure 5.9: Transmitted force of the delivery catheter that is used in a sheep relatively to the pushing force

Bartosch et al. supports this finding by pointing out that the transmitted force by the delivery catheters is pushing against the artery wall which could induce injury or trauma to the artery walls [4]. Especially in the aortic arch where a 180 degree turn has to be made. The delivery catheter is guided through the arch by pushing the catheter upward. The nose cone scrapes against the artery wall and is deviated from a straight line into an angle by the arterial wall to facilitate the bending of the delivery catheter. This pushing force, which is pointed out in figure 5.9, together with the scraping of the tip of the catheter can induce injury or trauma to the surrounding tissue [4].

5.3.4. Coaxial implantation

There is little information on the coaxial implantation of the prosthesis. Tay et al. state that embolization is the result of an oblique implantation to the annular valve, but there is little evidence in this statement [33]. Moreover, a lot of studies describe the dislocation of the valve during or after implantation, but not because of on oblique coordination. The main reason this doesn't return in the studies is the fact that the imaging techniques are in 2D. If the prosthesis is in an oblique coordination in the plane other then the plane that is visible during surgery, then this oblique coordination is not visible for the surgeons. A dislocation may be the result of an oblique implantation in the plane perpendicular to the imaging plane, but the cause will not be stated as an oblique implantation because that was not visible with the current imaging technique [29].

5.4. Results validation study

Error	Medtronics DS				Edwards DS				Prototype			
	X-axis(mm)	*Y-axis(mm)*	*Z-axis(mm)*	*Square Error*	*X-axis(mm)*	*Y-axis(mm)*	*Z-axis(mm)*	*Square Error*	*X-axis(mm)*	*Y-axis(mm)*	*Z-axis(mm)*	*Square Error*
Run 1	-3,5	6,2	-9,1	11,6	-1,0	-1,9	-9,1	9,4	-2,1	-1,9	-7,1	7,6
Run 2	-3,3	6,0	-9,9	12,0	-2,9	-3,5	-13,0	13,8	-3,3	-1,5	-5,0	6,2
Run 3	-2,8	6,5	-8,5	11,1	-3,1	-1,5	-12,3	12,8	-0,7	-1,6	-8,5	8,6
Run 4	-3,5	7,5	-7,1	10,9	-4,8	-0,3	-11,4	12,4	-2,0	-1,6	-7,5	7,9
Run 5	-3,4	7,1	-7,9	11,1	-2,9	-0,9	-8,9	9,4	-2,5	-3,6	-9,1	10,1
Mean Error	-3,3	6,7	-8,5	11,3	-2,9	-1,6	-10,9	11,6	-2,1	-2,0	-7,4	8,1

+

Figure 5.10: Table of location errors for each of the delivery systems compared to the reference point

Bibliography

[1] Jordi Alastruey, Nan Xiao, Henry Fok, Tobias Schaeffter, and C Alberto Figueroa. On the impact of modelling assumptions in multi-scale, subject-specific models of aortic haemodynamics. *Journal of The Royal Society Interface*, 13(119):20160073, 2016.

[2] Abdullah M Al Ali, Lukas Altwegg, Eric M Horlick, Christopher Feindel, Christopher R Thompson, Anson Cheung, Ronald G Carere, Karin Humphries, Jian Ye, Jean-Bernard Masson, et al. Prevention and management of transcatheter balloon-expandable aortic valve malposition. *Catheterization and Cardiovascular Interventions*, 72(4):573–578, 2008.

[3] V. Bapat and R. Attia. Transaortic Transcatheter Aortic Valve Implantation: Step-by-Step Guide. *Seminars in Thoracic and Cardiovascular Surgery*, 24(3), 2012.

[4] Marco Bartosch, Heiner Peters, Hendrik Spriestersbach, Darach O h Ici, Felix Berger, and Boris Schmitt. A Universal Delivery System for Percutaneous Heart Valve Implantation. *Annals of Biomedical Engineering*, 44(9):2683–2694, sep 2016.

[5] Christos V Bourantas, Nicolas M Van Mieghem, Vasim Farooq, Osama I Soliman, Stephan Windecker, Nicolo Piazza, and Patrick W Serruys. Future perspectives in transcatheter aortic valve implantation. *International journal of cardiology*, 168(1):11–18, 2013.

[6] Pak Hei Chan, Eduardo Alegria-Barrero, and Carlo Di Mario. Difficulties with horizontal aortic root in transcatheter aortic valve implantation. *Catheterization and Cardiovascular Interventions*, 81(4):630–635, 2013.

[7] A. Cribier. Development of transcatheter aortic valve implantation (TAVI): A heart-warming adventure. *European Geriatric Medicine*, 4(6), 2013.

[8] Peter PT de Jaegere. How to move toward the least invasive transfemoral transcatheter aortic valve implantation procedure? *Circulation: Cardiovascular Interventions*, 7(4):439–440, 2014.

[9] D Dvir, I Lavi, H Eltchaninoff, D Himbert, Y Almagor, F Descoutures, A Vahanian, C Tron, A Cribier, and R Kornowski. Multicenter Evaluation of Edwards SAPIEN Positioning During Transcatheter Aortic Valve Implantation With Correlates for Device Movement During Final Deployment. *Jacc-Cardiovascular Interventions*, 5(5):563–570, 2012.

[10] Thomas Pilgrim E. Guérios, Steffen Gloekler et al. Second valve implantation for the treatment of a malpositioned transcatheter aortic valve. *JIC: Journal of invasive Cardiology*, 24(9), 2012.

[11] Gry Wisthus Eveborn, Henrik Schirmer, Geir Heggelund, Per Lunde, and Knut Rasmussen. The evolving epidemiology of valvular aortic stenosis. the tromsø study. *Heart*, 99(6):396–400, 2013.

[12] Timothy A Fairbairn, John P Greenwood, and Daniel J Blackman. Multiple cerebral emboli following dislocation and retraction of a partially deployed corevalve prosthesis during transcatheter aortic valve implantation. *Catheterization and Cardiovascular Interventions*, 82(7):E911–E914, 2013.

[13] S. Geisbüsch, S. Bleiziffer, D. Mazzitelli, H. Ruge, R. Bauernschmitt, and R Lange. Incidence and Management of CoreValve Dislocation During Transcatheter Aortic Valve Implantation. *Circulation-Cardiovascular Interventions*, 3(6):531–536, 2010.

[14] P. Généreux, S.J. J Head, D.A. A Wood, S.K. K Kodali, M.R. R Williams, J.-M. M Paradis, M. Spaziano, A.P. P Kappetein, J.G. G Webb, A. Cribier, M.B. B Leon, S.J. J Head, D.A. A Wood, S.K. K Kodali, M.R. R Williams, J.-M. M Paradis, M. Spaziano, A.P. P Kappetein, J.G. G Webb, A. Cribier, and M.B. B Leon. Transcatheter aortic valve implantation 10-year anniversary: review of current evidence and clinical implications. *European Heart Journal*, 33(19):2388–+, 2012.

[15] Elliott M Groves, Ahmad Falahatpisheh, Jimmy L Su, and Arash Kheradvar. The Effects of Positioning of Transcatheter Aortic Valves on Fluid Dynamics of the Aortic Root. *ASAIO Journal*, 60:545–552, 2014.

[16] Mir A Imran, Mark L Pomeranz, and Brian A Glynn. Steerable catheter with adjustable bend location and/or radius and method, February 21 1995. US Patent 5,391,147.

[17] D.P. Jones, D.C. Leach, and D.R. Moore. Mechanical properties of poly(ether-etherketone)for engineering applications. *Polymer*, 26, 1985.

[18] Arthur F.Dalley Keith L.Moore. *Clinically Oriented Anatomy*. 6th Edition. Lippincott Williams And Wilkins, 2009.

[19] G.D. Lenders, V. Collas, J.M. Hernandez, V. Legrand, H.D. Danenberg, P. Den Heijer, I.E. Rodrigus, B.P. Paelinck, C.J. Vrints, and J.M. Bosmans. Depth of valve implantation, conduction disturbances and pacemaker implantation with CoreValve and CoreValve Accutrak system for Transcatheter Aortic Valve Implantation, a multi-center study. *International Journal of Cardiology*, 176(3), 2014.

[20] Raj R Makkar, Gregory P Fontana, Hasan Jilaihawi, Samir Kapadia, Augusto D Pichard, Pamela S Douglas, Vinod H Thourani, Vasilis C Babaliaros, John G Webb, Howard C Herrmann, et al. Transcatheter aortic-valve replacement for inoperable severe aortic stenosis. *New England Journal of Medicine*, 366(18):1696–1704, 2012.

[21] Raj R Makkar, Hasan Jilaihawi, Tarun Chakravarty, Gregory P Fontana, Samir Kapadia, Vasilis Babaliaros, Wen Cheng, Vinod H Thourani, Joseph Bavaria, Lars Svensson, et al. Determinants and outcomes of acute transcatheter valve-in-valve therapy or embolization: a study of multiple valve implants in the us partner trial (placement of aortic transcatheter valve trial edwards sapien transcatheter heart valve). *Journal of the American College of Cardiology*, 62(5):418–430, 2013.

[22] Jean-Bernard Masson, Jan Kovac, Gerhard Schuler, Jian Ye, Anson Cheung, Samir Kapadia, Murat E Tuzcu, Susheel Kodali, Martin B Leon, and John G Webb. Transcatheter Aortic Valve Implantation Review of the Nature, Management, and Avoidance of Procedural Complications. *JCIN*, 2:811–820.

[23] Gaspar Mestres, Marvin E Garcia, Xavier Yugueros, Rodrigo Urrea, Paolo Tripodi, Fernando Gomez, Jordi Maeso, and Vincent Riambau. Aortic arch and thoracic aorta curvature remodeling after thoracic endovascular aortic repair. *Annals of vascular surgery*, 38:233–241, 2017.

[24] Fabian Nietlispach, Namal Wijesinghe, David Wood, Ronald G Carere, and John G Webb. Current balloon-expandable transcatheter heart valve and delivery systems. *Catheterization and Cardiovascular Interventions*, 75(2):295–300, 2010.

[25] Rutger-Jan Nuis, Nicolas M Van Mieghem, Carl J Schultz, Apostolos Tzikas, Robert M Van der Boon, Anne-Marie Maugenest, Jin Cheng, Nicolo Piazza, Ron T Van Domburg, Patrick W Serruys, et al. Timing and potential mechanisms of new conduction abnormalities during the implantation of the medtronic corevalve system in patients with aortic stenosis. *European heart journal*, page ehr110, 2011.

[26] S.H. Ong, R. Mueller, and U. Gerckens. Sequential corevalve implantation for a mal-positioned prosthesis during transcatheter aortic valve implantation. *Catheterization and Cardiovascular Interventions*, 77(7), 2011.

[27] Anna Sonia Petronio, Marco De Carlo, Francesco Bedogni, Antonio Marzocchi, Silvio Klugmann, Francesco Maisano, Angelo Ramondo, Gian Paolo Ussia, Federica Ettori, Arnaldo Poli, et al. Safety and efficacy of the subclavian approach for transcatheter aortic valve implantation with the corevalve revalving systemclinical perspective. *Circulation: Cardiovascular Interventions*, 3(4):359–366, 2010.

[28] Alban Redheuil, Wen-Chung Yu, Elie Mousseaux, Ahmed A Harouni, Nadjia Kachenoura, Colin O Wu, David Bluemke, and Joao AC Lima. cg. *Journal of the American College of Cardiology*, 58(12):1262–1270, 2011.

[29] J Rodes-Cabau. Progress in Transcatheter Aortic Valve Implantation. *Revista Espanola De Cardiologia*, 63(4):439–450, 2010.

[30] Raphael Rosenhek, Bernard Iung, Pilar Tornos, Manuel J Antunes, Bernard D Prendergast, Catherine M Otto, Arie Pieter Kappetein, Janina Stepinska, Jens J Kaden, Christoph K Naber, et al. Esc working group on valvular heart disease position paper: assessing the risk of interventions in patients with valvular heart disease. *European heart journal*, 33(7):822–828, 2012.

[31] Patrick W Serruys, Nicolo Piazza, Alain Cribier, John G Webb, Jean-Claude Laborde, and Peter de Jaegere. *Transcatheter aortic valve implantation: tips and tricks to avoid failure*. CRC Press, 2009.

[32] S. Stortecky, L. Buellesfeld, P. Wenaweser, and S. Windecker. Transcatheter aortic valve implantation: The procedure. *Heart*, 98(SUPPL. 4), 2012.

[33] Edgar LW Tay, Ronen Gurvitch, Namal Wijeysinghe, Fabian Nietlispach, Jonathon Leipsic, David A Wood, Gerald Yong, Anson Cheung, Jian Ye, Samuel V Lichtenstein, et al. Outcome of patients after transcatheter aortic valve embolization. *JACC: Cardiovascular Interventions*, 4(2):228–234, 2011.

[34] M Thielmann, P Kahlert, T Konorza, R Erbel, H Jakob, D Wendt, · P Kahlert, · T Konorza, · R Erbel, · H Jakob, and · D Wendt. Current developments in transcatheter aortic valve implantation techniques. *Herz*, 36:696–705, 2011.

[35] Gian Paolo Ussia, Marco Barbanti, Kunal Sarkar, Patrizia Aruta, Marilena Scarabelli, Valeria Cammalleri, Sebastiano Imme, Anna Maria Pistritto, Simona Gulino, Massimiliano Mule, et al. Transcatheter aortic bioprosthesis dislocation: technical aspects and midterm follow-up. *EuroIntervention: journal of EuroPCR in collaboration with the Working Group on Interventional Cardiology of the European Society of Cardiology*, 7(11):1285–1292, 2012.

[36] Alec Vahanian, Ottavio Alfieri, Felicita Andreotti, Manuel J Antunes, Gonzalo Barón-Esquivias, Helmut Baumgartner, Michael Andrew Borger, Thierry P Carrel, Michele De Bonis, Arturo Evangelista, et al. Guidelines on the management of valvular heart disease. *European heart journal*, 33(19):2451–2496, 2012.

[37] John Webb, Josep Rodés-Cabau, Stephen Fremes, Philippe Pibarot, Marc Ruel, Reda Ibrahim, Robert Welsh, Christopher Feindel, and Samuel Lichtenstein. Transcatheter aortic valve implantation: a canadian cardiovascular society position statement. *Canadian Journal of Cardiology*, 28(5):520–528, 2012.

[38] Emma Wilton and Marjan Jahangiri. Post-stenotic aortic dilatation. *Journal of cardiothoracic surgery*, 1(1):7, 2006.

[39] Michael Želízko. Tavi–from patient selection to follow-up. *Cor et Vasa*, 2017.